AD-A059 808 AIR FORCE INST OF TECH WRIGHT-PATTERSON AFB OHIO F/G 20/11
STRESS ANALYSIS OF A RIGID BLOCK EMBEDDED IN AN ELASTIC HALF SP--ETC(U)
AUG 78 G K HARITOS
UNCLASSIFIED AFIT-CI-78-119 NL

END
DATE FILMED
12-78
DDC

UNCLASSIFIED

SECURITY CLASSIFICATION OF THIS PAGE (When Data Entered)

AD A059808

DDC FILE COPY

REPORT DOCUMENTATION PAGE

READ INSTRUCTIONS BEFORE COMPLETING FORM

1. REPORT NUMBER: AFIT-CI-78-119	2. GOVT ACCESSION NO.
3. RECIPIENT'S CATALOG NUMBER	
4. TITLE (and Subtitle): Stress Analysis of a Rigid Block Embedded in an Elastic Half Space.	5. TYPE OF REPORT & PERIOD COVERED: Dissertation
	6. PERFORMING ORG. REPORT NUMBER
7. AUTHOR(s): George Konstantinos Haritos	8. CONTRACT OR GRANT NUMBER(s): Doctoral thesis
9. PERFORMING ORGANIZATION NAME AND ADDRESS: AFIT student at Northwestern University, Evanston, Illinois	10. PROGRAM ELEMENT, PROJECT, TASK AREA & WORK UNIT NUMBERS
11. CONTROLLING OFFICE NAME AND ADDRESS: AFIT/CI, WPAFB OH 45433	12. REPORT DATE: 1978
	13. NUMBER OF PAGES: 84 Pages
14. MONITORING AGENCY NAME & ADDRESS (if different from Controlling Office)	15. SECURITY CLASS. (of this report): Unclassified
	15a. DECLASSIFICATION/DOWNGRADING SCHEDULE

16. DISTRIBUTION STATEMENT (of this Report)

Approved for Public Release, Distribution Unlimited

17. DISTRIBUTION STATEMENT (of the abstract entered in Block 20, if different from Report)

DDC RECEIVED OCT 4 1978 F

18. SUPPLEMENTARY NOTES

SEP 22 1978

JOSEPH P. HIPPS, Major, USAF
Director of Information, AFIT

APPROVED FOR PUBLIC RELEASE AFR 190-17.

19. KEY WORDS (Continue on reverse side if necessary and identify by block number)

20. ABSTRACT (Continue on reverse side if necessary and identify by block number)

012 200

DD FORM 1 JAN 73 1473 EDITION OF 1 NOV 65 IS OBSOLETE

UNCLASSIFIED

SECURITY CLASSIFICATION OF THIS PAGE (When Data Entered)

78-119D

NORTHWESTERN UNIVERSITY

STRESS ANALYSIS OF A RIGID BLOCK EMBEDDED IN AN ELASTIC HALF SPACE

A DISSERTATION

SUBMITTED TO THE GRADUATE SCHOOL

IN PARTIAL FULFILLMFNT OF THE REQUIREMENTS

for the degree

DOCTOR OF PHILOSOPHY

Field of Structural Mechanics

by

GEORGE KONSTANTINOS HARITOS

Evanston, Illinois

August 1978

To

My Parents, Konstantinos and Maria

and

My Wife and Son, Mary and Dino

ACKNOWLEDGEMENTS

The author expresses his gratitude to Professor Leon M. Keer who suggested the problems, and provided encouragement and guidance through all stages of research, and during the preparation of this dissertation.

Financial support in the form of a Walter P. Murphy Fellowship is gratefully acknowledged.

Finally, the author is grateful to the United States Air Force for affording him the opportunity to further his education.

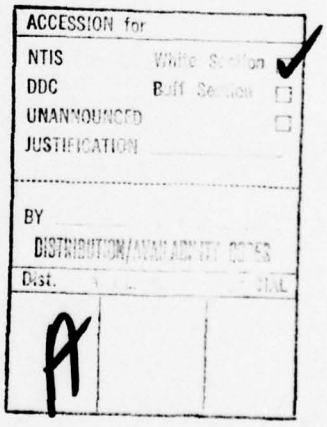

ABSTRACT

This dissertation investigates the plane elasticity problem of a finite, rigid rectangular block partially embedded in, and perfectly bonded to an elastic half space. The bond thickness is assumed to be sufficiently thin, so that there is no discontinuity in the displacements of the bonded surfaces.

The problem is formulated by superposition of the solutions to the problems of horizontal and vertical line inclusions beneath an elastic half space, which are derived from integral transform techniques. Substitution of these results into the boundary conditions appropriate for the embedded block problem leads to a system of six coupled singular integral equations, whose unknowns are the normal and shear stress discontinuities between the bonded surfaces.

Three distinct sets of loads are applied to the embedded block, so that it either translates without rotation in the x- or y- direction, or rotates about an axis in the z-direction. In all three cases, by taking advantage of the symmetric nature of the problems, the number of the governing singular integral equations is reduced from six to four. These equations may be solved numerically by employing the collocation scheme introduced by Erdogan, Gupta, and Cook, provided that they be supplemented with four subsidiary conditions. The requirement for additional conditions is dictated by the order of the singularities at the corners of the block, established through an asymptotic expansion of the singular integral equations in the vicinity of these corners.

The problem of two vertical inclusions perpendicular to the free surface of the half space, and loaded in a manner analogous to the embedded block problem, is also formulated for each case. These problems, besides their also being of interest, provide a further estimate of the accuracy of the numerical results.

The numerical analysis was carried out for various geometries for the case of plane strain. Several important physical quantities are computed, such as the diffusion of the load from the block into the elastic half space, and the local stress distribution around the block, excluding the singular points.

TABLE OF CONTENTS

LIST OF TABLES

LIST OF FIGURES

CHAPTER I

INTRODUCTION

This dissertation is concerned with the stress analysis of an elastic half space, in which a perfectly bonded, rigid rectangular block is partially embedded. The bond thickness is assumed to be sufficiently thin so that the displacements of the bonded surfaces are continuous. Within this context the problem is one of plane strain and can be considered appropriate to calculations that involve the stress distributions around foundations where the out-of-plane dimensions are very large when compared with the length or width of the rectangle. Alternatively, the problem can be viewed as one of generalized plane stress analyzing the load diffusion from a finite, rigid rectangular insert, partially embedded within a semi-infinite sheet, where the axis of the insert is perpendicular to the edge of the sheet. The geometry and coordinate system for such a block is shown in Fig. 1, where μ is the shear modulus and κ is related to Poisson's ratio by $\kappa = 3 - 4\nu$ (plane strain) or $\kappa = (3-\nu)/(1+\nu)$ (plane stress), and ν is Poisson's ratio.

Problems such as the one considered here have had a long history, which is best summarized in a paper by Muki and Sternberg [1], who consider the diffusion of load from a transverse tension bar into a semi-infinite elastic sheet. They reconsider the problem initially posed by Reissner [2], who considered the load transfer from a transverse stringer, a finite segment of which overlaps with,

and is continuously bonded to, a semi-infinite elastic sheet. Theirs is essentially a contact problem in which the finite stringer is attached to the semi-infinite sheet and their objective is to obtain a systematic reduction of the problem to a Fredholm integral equation via two contact models: i.e. line-contact or area-contact.

The present analysis differs from theirs in that the sheet is assumed to be cut so that it has a finite rectangular notch at its surface. A perfectly matching rigid, rectangular insert is then bonded within this notch.

Loading is applied to this embedded insert so that it either translates without rotation in the vertical or horizontal direction, or rotates due to an applied moment. The plane strain case corresponds to an infinite, rectangular block embedded within an elastic half space undergoing vertical or horizontal translation, or rotation.

It should be noted that Muki and Sternberg have also dealt with the three-dimensional problem of load diffusion from an axially loaded rod to a half space [3,4]. In [3] the problem of the axial force decay in an infinite cylindrical elastic bar bonded to an infinite medium is dealt with. An approximate solution scheme for cross-sections of arbitrary shape is developed and compared to the exact one for the case of a circular bar. This scheme is then used in [4] to solve the problem of load diffusion from a bar of arbitrary uniform cross-section partially embedded in, and bonded to a semi-infinite solid.

The solution of the considered problem is developed in successive stages. In Chapter II Green's functions are established for a horizontal and vertical line load beneath an elastic half space.

This formulation allows the boundary value problem to be written as having boundary conditions only on the surface of the notch. The results are derived using integral transform techniques, but they can also be derived by other methods. The primary references used for these derivations were the book by Sneddon [5], and the tables edited by Erdélyi [6].

Chapter III deals with the vertical translation of the finite rigid rectangular block partially embedded in, and perfectly bonded to an elastic half space, under an applied load 2P acting in the negative y-direction. The appropriate boundary conditions are written by superposing the horizontal and vertical inclusion results. The boundary conditions become the data for a system of singular integral equations, which can be solved numerically. It is noted that there are four points on the block that are singular: the intersection of the block with the free surface, $(\pm c,0)$, and the lower corners of the block, $(\pm c,h)$. These singularities can be accounted for in the analysis by the establishment of appropriate corner conditions through an asymptotic expansion of the governing singular integral equations in the vicinity of these singularities. It should be noted here that the solution of the transcedental equation derived for the corners $(\pm c,h)$ leads to two negative roots. Therefore, they both lead to singular contributions. The singular stress field is dominated by the largest singularity, and this is the one used in the present analysis. To the author's knowledge, the only work that considers both negative roots at a corner such as the one encountered here, is a paper by Westmann, [7], which deals with a wedge bonded to a half plane along

a finite length. The solution for that problem was developed using Mellin transforms, and numerical results were obtained by use of a modified finite difference method. However, accounting for both negative roots is beyond the scope of this dissertation. Finally, in order to obtain a further estimate of the accuracy of the numerical results, an analogous problem is formulated. This is the problem of two rigid vertical inclusions of length equal to the sides of the rigid block, and separated by a distance equal to the base of the block, partially embedded in and bonded to an elastic half space, each loaded by P in the negative y-direction.

The case of horizontal displacement of the rigid block loaded by 2Q, acting in the negative x-direction, and a moment M is considered in Chapter IV. The analogous case for the two inclusion problem is also examined in the same chapter.

Chapter V investigates the rotation of the rigid block under the action of a moment M. The two inclusion problem subjected to analogous loading is also formulated in that chapter.

In Chapter VI the method for obtaining numerical results is discussed. The collocation scheme introduced by Erdogan, Gupta, and Cook [8] is used to solve the system of singular integral equations governing each of the problems formulated in Chapters III-V. The method of solution allows the calculation of certain important physical quantities such as the diffusion of load from the block into the elastic half space, and also the local stress distribution around the block, excluding the singular points.

CHAPTER II

FORMULATION AND BASIC EQUATIONS

HORIZONTAL INCLUSION IN A HALF SPACE

The equations to be obtained here are for a bonded, rigid inclusion of length 2c located at a depth h beneath the free surface, y = 0, of an elastic half space. The inclusion is assumed to have zero thickness and its geometry and coordinate system are shown in Fig. 2. If the discontinuities in the normal and shear stresses are designated by A(x) and B(x), respectively, then the following conditions must be satisfied:

$$\begin{aligned} \tau_{yy}^{(2)} - \tau_{yy}^{(1)} &= A(x) \\ \tau_{xy}^{(2)} - \tau_{xy}^{(1)} &= B(x) \end{aligned} \qquad y = h,\ -c \leq x \leq c. \tag{2.1}$$

In addition to the above equations, the following continuity and boundary conditions must be satisfied:

$$\begin{aligned} u_x^{(2)} - u_x^{(1)} &= 0 \\ u_y^{(2)} - u_y^{(1)} &= 0 \end{aligned} \qquad y = h,\ -c \leq x \leq c \tag{2.2}$$

$$\tau_{yy}(x,0) = \tau_{xy}(x,0) = 0, \qquad 0 \leq |x| < \infty \tag{2.3}$$

where the superscripts (1), (2) define the regions above and below the inclusion.

In terms of the stress discontinuities, A(x) and B(x) defined above, the displacement derivatives and stresses throughout the half space are given as

$$\frac{\partial u_x^I}{\partial x}(x,y) = \frac{1}{4\pi(\kappa+1)\mu}\left\{\int_{-c}^{c} A(s)K_{N1}(x,y;s)ds + \int_{-c}^{c} B(s)K_{S1}(x,y;s)ds\right\} \tag{2.4}$$

$$\frac{\partial u_y^I}{\partial x}(x,y) = \frac{1}{4\pi(\kappa+1)\mu}\left\{\int_{-c}^{c} A(s)K_{N2}(x,y;s)ds + \int_{-c}^{c} B(s)K_{S2}(x,y;s)ds\right\} \tag{2.5}$$

$$\frac{\partial u_x^I}{\partial y}(x,y) = \frac{1}{4\pi(\kappa+1)\mu}\left\{\int_{-c}^{c} A(s)K_{N3}(x,y;s)ds + \int_{-c}^{c} B(s)K_{S3}(x,y;s)ds\right\} \tag{2.6}$$

$$\frac{\partial u_y^I}{\partial y}(x,y) = \frac{1}{4\pi(\kappa+1)\mu}\left\{\int_{-c}^{c} A(s)K_{N4}(x,y;s)ds + \int_{-c}^{c} B(s)K_{S4}(x,y;s)ds\right\} \tag{2.7}$$

$$\tau_{xx}^I(x,y) = \frac{1}{2\pi(\kappa+1)}\left\{\int_{-c}^{c} A(s)K_{N5}(x,y;s)ds + \int_{-c}^{c} B(s)K_{S5}(x,y;s)ds\right\} \tag{2.8}$$

$$\tau_{yy}^I(x,y) = \frac{1}{2\pi(\kappa+1)}\left\{\int_{-c}^{c} A(s)K_{N6}(x,y;s)ds + \int_{-c}^{c} B(s)K_{S6}(x,y;s)ds\right\} \tag{2.9}$$

$$\tau_{xy}(x,y) = \frac{1}{2\pi(\kappa+1)}\left\{\int_{-c}^{c} A(s)K_{N7}(x,y;s)ds + \int_{-c}^{c} B(s)K_{S7}(x,y;s)ds\right\} \tag{2.10}$$

The functions K_{Ni} and K_{Si}, $i = 1,2,\ldots,7$, are given in Appendix A and they are rational functions of x and y with both numerators and denominators being polynomials in x and y.

Equations (2.4) - (2.10) were derived using integral transform techniques [5,6], but they can also be derived by other methods.

VERTICAL INCLUSION IN A HALF SPACE

Here, the case of a vertical inclusion of length (b - a) perpendicular to the free surface of an elastic half space, y = 0, is solved (Fig. 2). Let the jumps in the normal and shear stresses across the inclusion be C(y) and D(y), respectively; then, the following relationships must hold:

$$\left.\begin{aligned} \tau_{xx}^{(2)} - \tau_{xx}^{(1)} &= C(y) \\ \tau_{xy}^{(2)} - \tau_{xy}^{(1)} &= D(y) \end{aligned}\right\} \quad x = c,\ a \le y \le b; \tag{2.11}$$

$$\left.\begin{aligned} u_x^{(2)} - u_x^{(1)} &= 0 \\ u_y^{(2)} - u_y^{(1)} &= 0 \end{aligned}\right\} \quad x = c,\ a \le y \le b; \tag{2.12}$$

$$\tau_{yy}(x,0) = \tau_{xy}(x,0) = 0, \quad y = 0,\ 0 \le |x| < \infty. \tag{2.13}$$

For this case the superscripts (1), (2) refer to the regions to the left and right of the inclusion, respectively.

In terms of the stress jumps, C(y) and D(y), defined by Eqs. (2.11), the displacement derivatives and stresses within the half space are given as

$$\frac{\partial u_x^{II}}{\partial x}(x,y) = \frac{1}{4\pi(\kappa+1)\mu}\left\{\int_a^b C(t)L_{N1}(x,y;t)dt + \int_a^b D(t)L_{S1}(x,y;t)dt\right\} \tag{2.14}$$

$$\frac{\partial u_y^{II}}{\partial x}(x,y) = \frac{1}{4\pi(\kappa+1)\mu}\left\{\int_a^b C(t)L_{N2}(x,y;t)dt + \int_a^b D(t)L_{S2}(x,y;t)dt\right\} \tag{2.15}$$

$$\frac{\partial u_x^{II}}{\partial y}(x,y) = \frac{1}{4\pi(\kappa+1)\mu}\left\{\int_a^b C(t)L_{N3}(x,y;t)dt + \int_a^b D(t)L_{S3}(x,y;t)dt\right\} \tag{2.16}$$

$$\frac{\partial u_y^{II}}{\partial y}(x,y) = \frac{1}{4\pi(\kappa+1)\mu}\left\{\int_a^b C(t)L_{N4}(x,y;t)dt + \int_a^b D(t)L_{S4}(x,y;t)dt\right\} \tag{2.17}$$

$$\tau_{xx}^{II}(x,y) = = \frac{1}{2\pi(\kappa+1)}\left\{\int_a^b C(t)L_{N5}(x,y;t)dt + \int_a^b D(t)L_{S5}(x,y;t)dt\right\} \tag{2.18}$$

$$\tau_{yy}^{II}(x,y) = \frac{1}{2\pi(\kappa+1)}\left\{\int_a^b C(t)L_{N6}(x,y;t)dt + \int_a^b D(t)L_{S6}(x,y;t)dt\right\} \tag{2.19}$$

$$\tau_{xy}^{II}(x,y) = \frac{1}{2\pi(\kappa+1)}\left\{\int_a^b C(t)L_{N7}(x,y;t)dt + \int_a^b D(t)L_{S7}(x,y;t)dt\right\} \tag{2.20}$$

where the functions L_{Ni} and L_{Si}, $i = 1,2,\ldots,7$, are given in Appendix A. It is noted that the superscript II is used to identify displacement derivatives and stresses associated with the vertical inclusion at $x = c$, while I was used in connection with the horizontal inclusion located at $y = h$. To obtain the equations associated with a vertical inclusion of length $(b - a)$, located at $x = -c$, one replaces c by -c in Eqs. (A.15)-(A.28), C(t) by E(t), and D(t) by F(t) in Eqs. (2.14)-(2.20). For this case the superscript III will be used. These equations will not be listed here but will be incorporated in the following chapters.

CHAPTER III

STRESS ANALYSIS OF EMBEDDED BLOCK: VERTICAL DISPLACEMENT

VERTICAL TRANSLATION OF RIGID BLOCK

The results of the preceding chapter are now superposed to formulate the problem of a rigid block perfectly bonded to an elastic half space and loaded as shown in Fig. 1. The limits of integration for the vertical inclusions (solutions II and III) are taken as a = 0 and b = h (Fig. 2). The boundary conditions for this problem are given next:

$$\left.\begin{aligned} \frac{\partial u_x}{\partial x} &= \frac{\partial u_x^{I}}{\partial x}(x,h) + \frac{\partial u_x^{II}}{\partial x}(x,h) + \frac{\partial u_x^{III}}{\partial x}(x,h) = 0 \\ \frac{\partial u_y}{\partial x} &= \frac{\partial u_y^{I}}{\partial x}(x,h) + \frac{\partial u_y^{II}}{\partial x}(x,h) + \frac{\partial u_y^{III}}{\partial x}(x,h) = 0 \end{aligned}\right\}, \quad -c \le x \le c, \; y = h; \tag{3.1}$$

$$\left.\begin{aligned} \frac{\partial u_x}{\partial y} &= \frac{\partial u_x^{I}}{\partial y}(-c,y) + \frac{\partial u_x^{II}}{\partial y}(-c,y) + \frac{\partial u_x^{III}}{\partial y}(-c,y) = 0 \\ \frac{\partial u_y}{\partial y} &= \frac{\partial u_y^{I}}{\partial y}(-c,y) + \frac{\partial u_y^{II}}{\partial y}(-c,y) + \frac{\partial u_y^{III}}{\partial y}(-c,y) = 0 \end{aligned}\right\}, \quad 0 \le y \le h, \; x = -c; \tag{3.2}$$

$$\left.\begin{aligned} \frac{\partial u_x}{\partial y} &= \frac{\partial u_x^{I}}{\partial y}(c,y) + \frac{\partial u_x^{II}}{\partial y}(c,y) + \frac{\partial u_x^{III}}{\partial y}(c,y) = 0 \\ \frac{\partial u_y}{\partial y} &= \frac{\partial u_y^{I}}{\partial y}(c,y) + \frac{\partial u_y^{II}}{\partial y}(c,y) + \frac{\partial u_y^{III}}{\partial y}(c,y) = 0 \end{aligned}\right\}, \quad 0 \le y \le h, \; x = c. \tag{3.3}$$

Equations (3.1)-(3.3) represent a system of six singular integral equations, which are given next:

$$\int_{-c}^{c} A(s)K_{N1}(x,h;s)ds + \int_{-c}^{c} B(s)K_{S1}(x,h;s)ds + \int_{0}^{h} C(t)L_{N1}(x,h;t)dt$$

$$+ \int_{0}^{h} D(t)L_{S1}(x,h;t)dt + \int_{0}^{h} E(t)\bar{L}_{N1}(x,h;t)dt + \int_{0}^{h} F(t)\bar{L}_{S1}(x,h;t)dt = 0,$$

$$-c \le x \le c; \qquad (3.4)$$

$$\int_{-c}^{c} A(s)K_{N2}(x,h;s)ds + \int_{-c}^{c} B(s)K_{S2}(x,h;s)ds + \int_{0}^{h} C(t)L_{N2}(x,h;t)dt$$

$$+ \int_{0}^{h} D(t)L_{S2}(x,h;t)dt + \int_{0}^{h} E(t)\bar{L}_{N2}(x,h;t) + \int_{0}^{h} F(t)\bar{L}_{S2}(x,h;t)dt = 0,$$

$$-c \le x \le c; \qquad (3.5)$$

$$\int_{-c}^{c} A(s)K_{N3}(-c,y;s)ds + \int_{-c}^{c} B(s)K_{S3}(-c,y;s)ds + \int_{0}^{h} C(t)L_{N3}(-c,y;t)dt$$

$$+ \int_{0}^{h} D(t)L_{S3}(-c,y;t)dt + \int_{0}^{h} E(t)\bar{L}_{N3}(-c,y;t)dt = 0, \quad 0 \le y \le h; \qquad (3.6)$$

$$\int_{-c}^{c} A(s)K_{N4}(-c,y;s)ds + \int_{-c}^{c} B(s)K_{S4}(-c,y;s)ds + \int_{0}^{h} C(t)L_{N4}(-c,y;t)dt$$

$$+ \int_{0}^{h} D(t)L_{S4}(-c,y;t)dt + \int_{0}^{h} F(t)\bar{L}_{S4}(-c,y;t)dt = 0, \quad 0 \le y \le h; \qquad (3.7)$$

$$\int_{-c}^{c} A(s)K_{N3}(c,y;s)ds + \int_{-c}^{c} B(s)K_{S3}(c,y;s)ds + \int_{0}^{h} C(t)L_{N3}(c,y;t)dt$$

$$+ \int_{0}^{h} E(t)\bar{L}_{N3}(c,y;t)dt + \int_{0}^{h} F(t)\bar{L}_{S3}(c,y;t)dt = 0, \quad 0 \le y \le h; \qquad (3.8)$$

$$\int_{-c}^{c} A(s)K_{N4}(c,y;s)ds + \int_{-c}^{c} B(s)K_{S4}(c,y;s)ds + \int_{0}^{h} D(t)L_{S4}(c,y;t)dt$$

$$+ \int_{0}^{h} E(t)\bar{L}_{N4}(c,y;t)dt + \int_{0}^{h} F(t)\bar{L}_{S4}(c,y;t)dt = 0, \quad 0 \le y \le h. \qquad (3.9)$$

The barred kernels $\bar{L}_{Ni}$ and $\bar{L}_{Si}$, $i = 1,2,\ldots,4$, are readily obtained from the corresponding unbarred kernels given in Appendix A by replacing c by -c. It is also noted that the boundary conditions for the integral

equations are homogeneous. However, the input data will be given in the form of subsidiary conditions that involve the load 2P applied to the block and the constraints, when the symmetry appropriate to the considered problem is used.

Since Eqs. (3.4)-(3.9) deal with the geometry of corners, their limit near the corners must produce relationships which hold true in the neighborhood of such corners. These relationships may be directly obtained from the governing singular integral equations, after the contributing parts are isolated from the entire equations. First, the order of the singularity at the intersection of the free surface with a vertical inclusion will be established by considering the appropriate contributory terms. Adjusting the coordinate system to account for the right-hand inclusion, the terms leading to the determination of the singularity at the free surface are given as

$$\int_0^h C(t)\left[\frac{2\kappa}{y-t} + \frac{\kappa^2+1}{y+t} + \frac{4t(y-t)}{(y+t)^3}\right]dt = 0, \tag{3.10}$$

where y is approaching zero. A second equation, identical to (3.10), is obtained for D(t). Assuming solutions of the form,

$$C(t) = \bar{C}(t)t^{\eta-1}, \quad D(t) = \bar{D}(t)t^{\eta-1}, \tag{3.11), (3.12}$$

where $0 < \eta < 1$, the following eigenvalue equation is deduced for the determination of η:

$$\sin^2\left(\frac{\pi\eta}{2}\right) = \frac{(\kappa+1)^2}{4} - \frac{1}{\kappa}\eta^2. \tag{3.13}$$

Except for a minor change in notation, Eq. (3.13) is identical to that determined by Williams [9] for a right-angle corner of an elastic plate in extension with fixed-free boundary conditions. When Eq. (3.13) is

solved for $\nu = 0.3$ (plane strain), the result is

$$\eta = 0.71117. \tag{3.14}$$

Conditions at the corners (c,h) and (-c,h) can be established in a similar manner through the use of Eqs. (3.4)-(3.9), where the following asymptotic forms are assumed for the sought functions:

$$A(s) = \bar{A}(s)(c^2 - s^2)^{\zeta-1}, \quad B(s) = \bar{B}(s)(c^2 - s^2)^{\zeta-1};$$

$$C(t) = \bar{C}(t)t^{\eta-1}(h - t)^{\zeta-1}, \ldots, F(t) = \bar{F}(t)t^{\eta-1}(h - t)^{\zeta-1} \tag{3.15}$$

where $0 < \zeta < 1$. The corner conditions for (c,h) are found to be

$$\kappa \cos(\pi\zeta)B_0 + (\kappa - \zeta)\cos(\tfrac{\pi\zeta}{2})C_0 + \zeta \sin(\tfrac{\pi\zeta}{2})D_0 = 0 \tag{3.16a}$$

$$\kappa \cos(\pi\zeta)A_0 + \zeta \sin(\tfrac{\pi\zeta}{2})C_0 + (\kappa + \zeta)\cos(\tfrac{\pi\zeta}{2})D_0 = 0 \tag{3.16b}$$

$$\zeta \sin(\tfrac{\pi\zeta}{2})A_0 + (\kappa + \zeta)\cos(\tfrac{\pi\zeta}{2})B_0 + \kappa \cos(\pi\zeta)C_0 = 0 \tag{3.16c}$$

$$(\kappa - \zeta)\cos(\tfrac{\pi\zeta}{2})A_0 + \zeta \sin(\tfrac{\pi\zeta}{2})B_0 + \kappa \cos(\pi\zeta)D_0 = 0, \tag{3.16d}$$

and for (-c,h)

$$\kappa \cos(\pi\zeta)B_0' + (\kappa - \zeta)\cos(\tfrac{\pi\zeta}{2})E_0 - \zeta \sin(\tfrac{\pi\zeta}{2})F_0 = 0 \tag{3.17a}$$

$$\kappa \cos(\pi\zeta)A_0' - \zeta \sin(\tfrac{\pi\zeta}{2})E_0 + (\kappa + \zeta)\cos(\tfrac{\pi\zeta}{2})F_0 = 0 \tag{3.17b}$$

$$(\kappa - \zeta)\cos(\pi\zeta)A_0' - \zeta \sin(\tfrac{\pi\zeta}{2})B_0' + \kappa \cos(\pi\zeta)F_0 = 0 \tag{3.17c}$$

$$-\zeta \sin(\tfrac{\pi\zeta}{2})A_0' + (\kappa + \zeta)\cos(\tfrac{\pi\zeta}{2})B_0' + \kappa \cos(\pi\zeta)E_0 = 0. \tag{3.17d}$$

In Eqs. (3.16) and (3.17) the following notation is used:

$$\begin{aligned} &A_0 = \bar{A}(c)(2c)^{\zeta-1}/h^{\eta-1}, \quad B_0 = \bar{B}(c)(2c)^{\zeta-1}/h^{\eta-1}, \\ &A_0' = \bar{A}(-c)(2c)^{\zeta-1}/h^{\eta-1}, \quad B_0' = \bar{B}(-c)(2c)^{\zeta-1}/h^{\eta-1}, \\ &C_0, D_0, E_0, F_0 = \bar{C}(h), \bar{D}(h), \bar{E}(h), \bar{F}(h). \end{aligned} \tag{3.18}$$

Equations (3.16) and (3.17) lead to the same eigenvalue equation, namely

$$\left[\kappa^2 \sin^2\left(\frac{3\pi\zeta}{2}\right) - \zeta^2\right]\left[\kappa^2 \sin^2\left(\frac{\pi\zeta}{2}\right) - \zeta^2\right] = 0, \tag{3.19}$$

where ζ is determined from

$$\sin\left(\frac{3\pi\zeta}{2}\right) = \pm \frac{1}{\kappa}\,\zeta, \tag{3.20}$$

which is in agreement with Williams' result for a fixed-fixed $3\pi/2$ - corner of an elastic plate in extension [9]. If the positive sign in Eq. (3.20) is chosen and $\nu = 0.3$ (plane strain), the result is

$$\zeta = 0.59516\,. \tag{3.21}$$

It should be noted that Eq. (3.20) with the negative sign also yields a root in the interval of interest, $\zeta = 0.75904$; however, since the numerical scheme used to obtain numerical results [8] can only accommodate one of these roots, the gravest one, given by Eq. (3.21) will be used.

Equations (3.4)-(3.9) represent a system of six singular integral equations, which along with appropriate subsidiary conditions can be solved for the six unknown stress discontinuities A(s), B(s), ..., F(t). However, by taking advantage of the symmetric nature of the problem, the number of unknowns can be reduced to <u>four</u>, since the following relationships must hold:

$$E(y) = -C(y),\quad F(y) = D(y). \tag{3.22}$$

Thus, the subsidiary conditions associated with equations (3.4)-(3.9) are not needed, and will not be listed here. Equation (3.22) is incorporated to write Eqs. (3.4)-(3.5), and (3.8)-(3.9) in the following form:

$$\int_{-c}^{c} A(s)K_{N1}(x,h;s)ds + \int_{-c}^{c} B(s)K_{S1}(x,h;s)ds$$

$$+ \int_{0}^{h} C(t)[L_{N1}(x,h;t) - \bar{L}_{N1}(x,h;t)]dt$$

$$+ \int_{0}^{h} D(t)[L_{S1}(x,h;t) + \bar{L}_{S1}(x,h;t)]dt = 0, \quad -c \leq x \leq c ; \tag{3.23}$$

$$\int_{-c}^{c} A(s)K_{N2}(x,h;s)ds + \int_{-c}^{c} B(s)K_{S2}(x,h;s)ds$$

$$+ \int_{0}^{h} C(t)[L_{N2}(x,h;t) - \bar{L}_{N2}(x,h;t)]dt$$

$$+ \int_{0}^{h} D(t)[L_{S2}(x,h;t) + \bar{L}_{S2}(x,h;t)]dt = 0, \quad -c \leq x \leq c ; \tag{3.24}$$

$$\int_{-c}^{c} A(s)K_{N3}(c,y;s)ds + \int_{-c}^{c} B(s)K_{S3}(c,y;s)ds$$

$$+ \int_{0}^{h} C(t)[L_{N3}(c,y;t) - \bar{L}_{N3}(c,y;t)]dt$$

$$+ \int_{0}^{h} D(t)\bar{L}_{S3}(c,y;t)dt = 0, \quad 0 \leq y \leq h ; \tag{3.25}$$

$$\int_{-c}^{c} A(s)K_{N4}(c,y;s)ds + \int_{-c}^{c} B(s)K_{S4}(c,y;s)ds$$

$$+ \int_{0}^{h} C(t)[-\bar{L}_{N4}(c,y;t)]dt$$

$$+ \int_0^h D(t)[L_{S4}(c,y;t) + \bar{L}_{S4}(c,y;t)]dt = 0 \quad 0 \leq y \leq h. \tag{3.26}$$

Note that Eqs. (3.6)-(3.7) are eliminated as unnecessary. It is also clear that A(x) must be symmetric and B(x) antisymmetric in the range $-c \leq x \leq c$. These properties will be incorporated in the numerical analysis.

Since the unknown stress discontinuities, A(s), B(s), C(t), and D(t), have integrable singularities at the end points, in addition to Eqs. (3.23)-(3.26), they must also satisfy the following subsidiary conditions [8]:

$$\int_{-c}^{c} A(x)dx + 2\int_0^h D(y)dy = 2P \ ; \tag{3.27}$$

$$\int_0^c \left[\frac{\partial u_x}{\partial x}\right]_{y=0} dx = 0 \ ; \tag{3.28}$$

$$\int_0^c \left[\frac{\partial u_y}{\partial x}\right]_{y=0} dx - \int_0^h \left[\frac{\partial u_y}{\partial y}\right]_{x=0} dy = 0 \ ; \tag{3.29}$$

$$B(0) = 0 \ . \tag{3.30}$$

The choice of Eqs. (3.27)-(3.30) as the subsidiary conditions appropriate for this problem warrants a brief discussion. It was found that extreme care must be exercised in selecting the correct combination of conditions from several available relationships which could, conceivably, serve as subsidiary conditions. The task is to prescribe conditions which supplement the boundary conditions in describing the problem, without using redundant ones, and, of course, without violating any of the elasticity rules that apply to mixed

boundary value problems. Including redundant conditions has the same effect as using the same equation twice (i.e. renders the matrix of coefficients singular), while the subtle manner in which certain factors enter the problem creates the danger of violating fundamental elasticity rules, such as overconstraining the problem by prescribing tractions and displacements along the same direction.

The governing singular integral equations (Eqs. 3.23 - 3.26) ensure that the base and the sides of the block do not rotate and do not elongage (shrink). Equation (3.27) represents the global equilibrium for the rigid block in the vertical direction. Equation (3.30) is a statement requiring $B(x)$ to be antisymmetric. This, along with Eq. (3.22) which requires that $E(y) = -C(y)$, satisfies the equation of equilibrium in the horizontal direction. Equations (3.28) and (3.29) impose kinematic restrictions on the problem. Equation (3.28) fixes the sides of the block at $x = \pm c$, while Eq. (3.29) requires that the base and the sides of the block do not move relative to each other in the vertical direction.

Equations (3.23)-(3.30) are therefore the relationships appropriate for the solution of the problem of a rigid block embedded in an elastic half space and undergoing vertical displacement.

THE TWO-INCLUSION PROBLEM: VERTICAL TRANSLATION

The integral equations associated with the vertical line inclusions embedded in an elastic half space, which were derived in Chapter II, are used in this section to formulate a problem which is analogous to the rigid block one, although much simpler. This is the problem of two inclusions of length h, parallel to each other, perpendicular to the free surface of the elastic half space and located at $x = c$ and $x = -c$, respectively. Furthermore, these two inclusions are thought of as being rigidly connected to each other above the surface, so that they cannot move relative to each other. A load P acting in the negative y-direction is applied to each of them, and they are to translate vertically without rotation.

The boundary conditions appropriate for this problem are given next:

$$\frac{\partial u_x}{\partial y} = \frac{\partial u_x^{II}}{\partial y}(c,y) + \frac{\partial u_x^{III}}{\partial y}(c,y) = 0$$

$$\frac{\partial u_y}{\partial y} = \frac{\partial u_y^{II}}{\partial y}(c,y) + \frac{\partial u_y^{III}}{\partial y}(c,y) = 0 \qquad , \ 0 \le y \le h, \ x = c \ ; \quad (3.31)$$

$$\frac{\partial u_x}{\partial y} = \frac{\partial u_x^{II}}{\partial y}(-c,y) + \frac{\partial u_x^{III}}{\partial y}(-c,y) = 0$$

$$\frac{\partial u_y}{\partial y} = \frac{\partial u_y^{II}}{\partial y}(-c,y) + \frac{\partial u_y^{III}}{\partial y}(-c,y) = 0 \qquad , \ 0 \le y \le h, \ x = -c. \quad (3.32)$$

Equations (3.31) - (3.32) represent a system of four singular integral equations. However, the symmetry conditions given in Eq. (3.22) also apply to the two-inclusion problem. Therefore, it is only necessary to solve for two of the unknown stress discontinuities.

Equation (3.22) and the results of Chapter II are incorporated to write Eqs. (3.31) in the following form:

$$\int_0^h C(t)[L_{N3}(c,y;t) - \bar{L}_{N3}(c,y;t)]dt + \int_0^h D(t)\,\bar{L}_{S3}(c,y;t)dt = 0,\ 0 \le y \le h; \tag{3.33}$$

$$\int_0^h C(t)[-\bar{L}_{N4}(c,y;t)]dt + \int_0^h D(t)[L_{S4}(c,y;t) + \bar{L}_{S4}(c,y;t)]dt = 0,$$

$$0 \le y \le h. \tag{3.34}$$

The kernels appearing in Eqs. (3.33)-(3.34) are as defined earlier.

Equations (3.33)-(3.34) may be solved for the unknown stress discontinuities, C(t) and D(t), provided that the subsidiary conditions listed next are satisfied:

$$\int_0^h D(y)dy = P; \tag{3.35}$$

$$\int_0^c [\frac{\partial u}{\partial x}]_{y=0} dx = 0. \tag{3.36}$$

The physical significance of Eqs. (3.35)-(3.36) is clear. Equation (3.35) is the equation of equilibrium in the y-direction, while Eq. (3.36) fixes the inclusions at $x = \pm c$. Note that the equation of equilibrium in the x-direction is also satisfied, since $E(t) = -C(t)$. Concerning the order of the singularities at $y = 0,h$, it should be noted here that while the one at the free surface, $(\pm c,0)$, remains unchanged and is determined from Eq. (3.14), $\eta = 0.71117$, the singularity at $(\pm c,h)$ appropriate for the two-inclusion problem is square root.

CHAPTER IV

STRESS ANALYSIS OF EMBEDDED BLOCK: HORIZONTAL DISPLACEMENT

HORIZONTAL TRANSLATION OF RIGID BLOCK

The problem investigated in this section is that of a rigid block partially embedded in an elastic half space and forced to translate in the negative x-direction without rotation, under the action of a horizontal load 2Q, and a moment M, as shown in Fig. 3.

The boundary conditions appropriate for this problem are the same as those given in Chapter III, Eqs. (3.1)-(3.3), for the vertical translation of the rigid block problem, and they are repeated next:

$$\frac{\partial u_x}{\partial x} = 0, \quad \frac{\partial u_y}{\partial x} = 0; \quad -c \leq x \leq c, \; y = h; \tag{4.1}$$

$$\frac{\partial u_x}{\partial y} = 0, \quad \frac{\partial u_y}{\partial y} = 0; \quad 0 \leq y \leq h, \; x = \pm c. \tag{4.2}$$

Equations (4.1) - (4.2) represent a system of six singular integral equations in the unknown stress discontinuities A(s), B(s), C(t), ..., F(t), which were defined in Chapter II. The symmetry of the problem requires that the following relationships hold:

$$E(y) = C(y), \; F(y) = -D(y); \tag{4.3}$$

$$A(x) = -A(-x), \; B(x) = B(-x). \tag{4.4}$$

Equation (4.3) reduces the number of unknowns from six to four, thereby allowing the elimination of two of the governing singular integral equations. Equation (4.4) will be incorporated in the numerical analysis.

Using Eq. (4.3) the four governing equations are now written in the following form:

$$\int_{-c}^{c} A(s)K_{N1}(x,h;s)ds + \int_{-c}^{c} B(s)K_{S1}(x,h;s)ds +$$

$$+ \int_{0}^{h} C(t)[L_{N1}(x,h;t) + \bar{L}_{N1}(x,h;t)]dt +$$

$$+ \int_{0}^{h} D(t)[L_{S1}(x,h;t) - \bar{L}_{S1}(x,h;t)]dt = 0, \; -c \leq x \leq c; \qquad (4.5)$$

$$\int_{-c}^{c} A(s)K_{N2}(x,h;s)ds + \int_{-c}^{c} B(s)K_{S2}(x,h;s)ds +$$

$$+ \int_{0}^{h} C(t)[L_{N2}(x,h;t) + \bar{L}_{N2}(x,h;t)]dt +$$

$$+ \int_{0}^{h} D(t)[L_{S2}(x,h;t) - \bar{L}_{S2}(x,h;t)]dt = 0, \; -c \leq x \leq c; \qquad (4.6)$$

$$\int_{-c}^{c} A(s)K_{N3}(c,y;s)ds + \int_{-c}^{c} B(s)K_{S3}(c,y;s)ds +$$

$$+ \int_{0}^{h} C(t)[L_{N3}(c,y;t) + \bar{L}_{N3}(c,y;t)]dt +$$

$$+ \int_{0}^{h} D(t)[-\bar{L}_{S3}(c,y;t)]dt = 0, \; 0 \leq y \leq h; \qquad (4.7)$$

$$\int_{-c}^{c} A(s)K_{N4}(c,y;s)ds + \int_{-c}^{c} B(s)K_{S4}(c,y;s)ds +$$

$$+ \int_{0}^{h} C(t)\bar{L}_{N4}(c,y;t)dt +$$

$$+ \int_{0}^{h} D(t)[L_{S4}(c,y;t) - \bar{L}_{S4}(c,y;t)]dt = 0, \ 0 \leq y \leq h. \qquad (4.8)$$

The kernels K_{Ni}, K_{Si}, L_{Ni}, and L_{Si}, $i = 1, \ldots, 4$, are given in Appendix A. The barred kernels $\bar{L}_{Ni}$, $\bar{L}_{Si}$, $i = 1, \ldots, 4$, are obtained from the corresponding unbarred kernels by replacing c by -c.

Note that the order of the singularities at the surface, $(\pm c,0)$, and at the corners, $(\pm c,h)$, remains unchanged and is as given in Chapter III, Eqs. (3.14) and (3.21). Of course, the same holds true for the corner conditions, and the ones appropriate for the corner (c,h) are given by Eq. (3.16).

Equations (4.5)-(4.8) can be solved for the unknown stress discontinuities A(s), B(s), C(t), and D(t), provided that a set of subsidiary conditions is also satisfied. The need for additional conditions is due to the fact that A(s), ..., D(t) have integrable singularities at the end points, as explained in Chapter III. The subsidiary conditions associated with Eqs. (4.5)-(4.8) are given next:

$$\int_{-c}^{c} B(x)dx + 2\int_{0}^{h} C(y)dy = 2Q \ ; \qquad (4.9)$$

$$\int_{0}^{c} \left[\frac{\partial u}{\partial x}\right]_{y=0} dx = 0 \ ; \qquad (4.10)$$

$$\int_0^c \left[\frac{\partial u_x}{\partial x}\right]_{y=0} dx - \int_0^h \left[\frac{\partial u_x}{\partial y}\right]_{x=0} dy = 0 \ ; \tag{4.11}$$

$$A(0) = 0 \ . \tag{4.12}$$

The discussion presented in Chapter III concerning the subsidiary conditions (3.27)-(3.30), also applies to the selection of Eqs. (4.9)-(4.12) as the correct set of conditions needed to supplement the governing singular integral equations, Eqs. (4.5)-(4.8), and will not be repeated here.

It suffices to state that Eqs. (4.9) and (4.12), the latter in association with Eq. (4.3), represent the global equations of equilibrium for the block in the x- and the y- directions, respectively. Equation (4.10) ensures that the sides of the block do not translate vertically, while Eq. (4.11) requires that the base and the sides of the block do not move relative to each other in the horizontal direction.

THE TWO-INCLUSION PROBLEM: HORIZONTAL TRANSLATION

In Chapter III the two-inclusion problem was described, and formulated for the vertical translation case. The present section considers the two-inclusion problem undergoing horizontal translation, under the action of a load 2Q in the negative x-direction. As previously, the rigid inclusions are thought of as being rigidly connected to each other above the surface, and they are to translate without rotation.

The boundary conditions for this problem are identical to the ones given by Eqs. (3.31)-(3.32), and are repeated next:

$$\frac{\partial u_x}{\partial y} = 0; \quad \frac{\partial u_y}{\partial y} = 0; \; 0 \leq y \leq h, \; x = \pm c \; . \tag{4.13}$$

The symmetry relationships given in Eq. (4.3) are incorporated to write the governing singular integral equations, at x = c, in the following form:

$$\int_0^h C(t)\,[L_{N3}(c,y;t) + \bar{L}_{N3}(c,y;t)]\,dt +$$

$$+ \int_0^h D(t)\,[-\bar{L}_{S3}(c,y;t)]\,dt = 0, \; 0 \leq y \leq h; \tag{4.14}$$

$$\int_0^h C(t)\,\bar{L}_{N4}(c,y;t)\,dt +$$

$$+ \int_0^h D(t)\,[L_{S4}(c,y;t) - \bar{L}_{S4}(c,y;t)]\,dt = 0, \; 0 \leq y \leq h. \tag{4.15}$$

The stress discontinuities C(t) and D(t) were defined in Chapter II, Eq. (2.11), while the kernels $L_{N3,4}$ and $L_{S3,4}$ are given in Appendix A. Recall that the barred kernels are obtained from the corresponding unbarred ones by replacing c by -c.

The functions being sought, C(t) and D(t), have integrable singularities at the end points; therefore, besides equations (4.14)-(4.15) they must also satisfy the following subsidiary conditions:

$$\int_0^h C(y)dy = Q \ ; \tag{4.16}$$

$$\int_0^c [\frac{\partial u}{\partial x}]_{y=0} \ dx = 0. \tag{4.17}$$

Equation (4.16) is the equation of equilibrium in the x-direction, while equilibrium in the y-direction is also satisfied by virtue of the symmetry of the problem, Eq. (4.3). Equation (4.17) requires that the rigid inclusions do not translate in the y-direction.

In regard to the order of the singularities for this problem, note that the singularity at $(\pm c,h)$ is square root, while that at the surface, $(\pm c,0)$, remains unchanged, $\eta = 0.71117$.

CHAPTER V

STRESS ANALYSIS OF EMBEDDED BLOCK: ROTATION

ROTATION OF RIGID BLOCK

This chapter investigates the problem of a partially embedded rigid block that rotates through an angle α under the action of a moment M, as shown in Fig. 3. Here, the tangential load Q is set equal to zero. The boundary conditions for this problem are given next:

$$\frac{\partial u_x}{\partial x} = 0, \quad \frac{\partial u_y}{\partial x} = \alpha; \quad -c \leq x \leq c, \quad y = h; \tag{5.1}$$

$$\frac{\partial u_x}{\partial y} = -\alpha, \quad \frac{\partial u_y}{\partial y} = 0; \quad 0 \leq y \leq h, \quad x = \pm c. \tag{5.2}$$

Substitution of the horizontal and vertical inclusion results derived in Chapter II in Eqs. (5.1)-(5.2) leads to a system of six governing singular integral equations with generalized Cauchy kernels. However, the symmetric nature of the problem allows for the elimination of two of the unknown stress discontinuities, since the relationships given next must be satisfied:

$$E(y) = C(y); \quad F(y) = -D(y). \tag{5.3}$$

Therefore, only four of the equations represented by Eqs. (5.1)-(5.2) are necessary for the solution to this problem. Note that the symmetry of the problem also requires that A(x) is antisymmetric, and B(x) symmetric in the range $-c \leq x \leq c$.

Equation (5.3) is incorporated to write the equations represented by Eq. (5.1) and those of (5.2) at $x = c$ in the following form:

$$\frac{1}{4\pi(\kappa+1)\mu}\left\{\int_{-c}^{c} A(s)K_{N1}(x,h;s)ds + \int_{-c}^{c} B(s)K_{S1}(x,h;s)ds\right.$$

$$+ \int_{0}^{h} C(t)[L_{N1}(x,h;t) + \bar{L}_{N1}(x,h;t)]dt$$

$$\left. + \int_{0}^{h} D(t)[L_{S1}(x,h;t) - \bar{L}_{S1}(x,h;t)]dt\right\} = 0, \quad -c \leq x \leq c; \qquad (5.4)$$

$$\frac{1}{4\pi(\kappa+1)\mu}\left\{\int_{-c}^{c} A(s)K_{N2}(x,h;s)ds + \int_{-c}^{c} B(s)K_{S2}(x,h;s)ds\right.$$

$$+ \int_{0}^{h} C(t)[L_{N2}(x,h;t) + \bar{L}_{N2}(x,h;t)]dt$$

$$\left. + \int_{0}^{h} D(t)[L_{S2}(x,h;t) - \bar{L}_{S2}(x,h;t)]dt\right\} = \alpha, \quad -c \leq x \leq c; \qquad (5.5)$$

$$\frac{1}{4\pi(\kappa+1)\mu}\left\{\int_{-c}^{c} A(s)K_{N3}(c,y;s)ds + \int_{-c}^{c} B(s)K_{S3}(c,y;s)ds\right.$$

$$+ \int_{0}^{h} C(t)[L_{N3}(c,y;t) + \bar{L}_{N3}(c,y;t)]dt$$

$$\left. + \int_{0}^{h} D(t)[-\bar{L}_{S3}(c,y;t)]dt\right\} = -\alpha, \quad 0 \leq y \leq h; \qquad (5.6)$$

$$\frac{1}{4\pi(\kappa+1)\mu}\{\int_{-c}^{c} A(s)K_{N4}(c,y;s)ds + \int_{-c}^{c} B(s)K_{S4}(c,y;s)$$

$$+ \int_{0}^{h} C(t)\bar{L}_{N4}(c,y;t)dt +$$

$$+ \int_{0}^{h} D(t)[L_{S4}(c,y;t) - \bar{L}_{S4}(c,y;t)]dt\} = 0, \quad 0 \leq y \leq h. \qquad (5.7)$$

The kernels appearing in Eqs. (5.4)-(5.7) are as defined previously. Note that the corner conditions for this problem are given by Eqs. (3.16), for the corner (c,h). The order of the singularities at the points $(\pm c,0)$, and $(\pm c,h)$ was derived previously, and is given by Eqs. (3.14) and (3.21), respectively.

The unknown functions A(s),B(s), C(t), and D(t) have integrable singularities at the end points. Thus, Eqs. (5.4)-(5.7) must be supplemented by additional conditions, and the ones appropriate for this problem are given next:

$$\int_{-c}^{c} B(x)dx + 2\int_{0}^{h} C(y)\,dy = 0\ ; \qquad (5.8)$$

$$\int_{0}^{c} [\frac{\partial u_y}{\partial x}]_{y=0}\,dx = c\alpha\ ; \qquad (5.9)$$

$$\int_{0}^{c} [\frac{\partial u_x}{\partial x}]_{y=0}\,dx - \int_{0}^{h} [\frac{\partial u_x}{\partial y}]_{x=0}\,dy = h\alpha\ ; \qquad (5.10)$$

$$A(0) = 0. \qquad (5.11)$$

Equation (5.8) represents the global equilibrium equation for the rigid block in the x-direction. Equilibrium in the y-direction is

satisfied by Eq. (5.11), which requires that A(x) is antisymmetric, in association with Eq. (5.3), requiring that F(y) = -D(y). Equations (5.9)-(5.10) impose kinematic restrictions on the problem. Equation (5.9) prescribes the translation of the corner (c,0) of the block in the y-direction, while Eq. (5.10) gives the relationship between the horizontal displacements of points (c,0) and (0,h) on the block. It should be noted that the usual small angle approximations have been employed in writing Eqs. (5.9)-(5.10).

THE TWO-INCLUSION PROBLEM: ROTATION

The problem considered in this section is that of two vertical rigid inclusions, partially embedded in an elastic half space and perfectly bonded to it, as described earlier in Chapter III, and loaded in such a manner, so that they both rotate through an angle α.

The boundary conditions for this problem are given next:

$$\frac{\partial u_x}{\partial y} = -\alpha, \quad \frac{\partial u_y}{\partial y} = 0; \quad 0 \leq y \leq h, \; x = \pm c. \tag{5.12}$$

The symmetry conditions given in Eq. (5.3) reduce the number of unknown stress discontinuities to two; hence, only two of the four singular integral equations represented by Eq. (5.12) are needed for a solution.

Equation (5.3) is used to write the equations governing this problem, at $x = c$, in the following form:

$$\frac{1}{4\pi(\kappa+1)\mu} \left\{ \int_0^h C(t)\,[L_{N3}(c,y;t) + \bar{L}_{N3}(c,y;t)]\,dt \right.$$

$$\left. + \int_0^h D(t)\,[-\bar{L}_{S3}(c,y;t)]\,dt \right\} = -\alpha, \quad 0 \leq y \leq h; \tag{5.13}$$

$$\frac{1}{4\pi(\kappa+1)\mu} \left\{ \int_0^h C(t)\,\bar{L}_{N4}(c,y;t)\,dt \right.$$

$$\left. + \int_0^h D(t)\,[L_{S4}(c,y;t) - \bar{L}_{S4}(c,y;t)]\,dt \right\} = 0, \; 0 \leq y \leq h. \tag{5.14}$$

Equations (5.13)-(5.14) may be solved for the unknown functions $C(t)$ and $D(t)$, provided that the subsidiary conditions given next are satisfied:

$$\int_0^h C(y)dy = 0 \quad ; \tag{5.15}$$

$$\int_0^c [\frac{\partial u_y}{\partial x}]_{y=0} dx = c\alpha \ . \tag{5.16}$$

Equation (5.15) is the equation of equilibrium in the x-direction, while Eq. (5.16) is identical to Eq. (5.9), which was written for the rigid block problem, and it prescribes the displacement in the y-direction of the point (c,0) of the block relative to the midpoint at the surface.

As in the previous cases of the two-inclusion problem, the singularities are of order $(\eta-1)$ at the surface points $(\pm c,0)$, and $(0.5-1)$ at the points $(\pm c,h)$, where $\eta = 0.71117$.

CHAPTER VI

NUMERICAL ANALYSIS AND DISCUSSION

NUMERICAL ANALYSIS

The objective of the numerical analysis is to solve numerically the systems of governing singular integral equations with the corresponding subsidiary conditions, derived in the previous three chapters, for the unknown stress discontinuities.

The equations are normalized by introducing the following variable changes:

$$x = c\bar{x}, \quad s = c\bar{s}; \tag{6.1}$$

$$y = \frac{h}{2}(1+\bar{y}), \quad t = \frac{h}{2}(1+\bar{t}). \tag{6.2}$$

In addition, the stress discontinuities are given forms that reflect their correct singularities at the corners (and the surface). For the case of vertical displacement of the rigid block the following substitutions are made:

$$A(s) = \frac{P}{c}\bar{A}(\bar{s})(1-\bar{s}^2)^{\zeta-1}; \quad B(s) = \frac{P}{c}\bar{B}(\bar{s})(1-\bar{s}^2)^{\zeta-1}; \tag{6.3}$$

$$C(t) = \frac{2P}{h}\bar{C}(\bar{t})(1-\bar{t})^{\zeta-1}(1+\bar{t})^{\eta-1};$$

$$D(t) = \frac{2P}{h}\bar{D}(\bar{t})(1-\bar{t})^{\zeta-1}(1+\bar{t})^{\eta-1}. \tag{6.4}$$

Equations (6.1)-(6.4) also apply to the horizontal translation of the rigid block problem, provided that P is replaced by Q. Note that Eqs. (6.2) and (6.4) are also employed to normalize the equations derived for the two-inclusion problem, for the vertical and horizontal translation cases.

To normalize the equations derived for the case of rotation of the rigid block (see Chapter V) the following substitutions are needed:

$$A(s) = \frac{2\pi(\kappa+1)\mu\alpha c}{\kappa} \bar{A}(\bar{s})(1-\bar{s}^2)^{\zeta-1};$$
$$B(s) = \frac{2\pi(\kappa+1)\mu\alpha c}{\kappa} \bar{B}(\bar{s})(1-\bar{s}^2)^{\zeta-1}; \tag{6.5}$$

$$C(t) = \frac{2\pi(\kappa+1)\mu\alpha h}{\kappa} \bar{C}(\bar{t})(1-\bar{t})^{\zeta-1}(1+\bar{t})^{\eta-1};$$
$$D(t) = \frac{2\pi(\kappa+1)\mu\alpha h}{\kappa} \bar{D}(\bar{t})(1-\bar{t})^{\zeta-1}(1+\bar{t})^{\eta-1}. \tag{6.6}$$

The substitutions given in Eqs. (6.1)-(6.2) also apply to this problem. Equations (6.2) and (6.6) are also used to normalize the equations associated with the two-inclusion problem undergoing rotation.

Equations (6.1)-(6.6) will appropriately normalize the governing singular integral equations and the subsidiary conditions so that the numerical analysis may be conducted. An adjustment is required in Eqs. (6.1) for normalizing Eqs. (3.28)-(3.29), (3.36), (4.10)-(4.11), (4.17), (5.9)-(5.10), and (5.16); instead of $x = c\bar{x}$, take

$$x = c(1+\bar{x})/2. \tag{6.7}$$

For convenience, the parameter γ is introduced, and is defined as

$$\gamma = c/h. \tag{6.8}$$

It should be noted that for the case of rotation of the rigid block, it becomes necessary to assign a specific numerical value to either c or h. Thus, for that problem h is given unit length, and therefore γ becomes equal to c.

The numerical scheme to be used in this analysis is that described in Erdogan, Gupta, and Cook [8], and is a collocation scheme based upon formulas for Gaussian integration (see Stroud and Secrest [10]). The integration points, $\bar{s}_i$, $\bar{t}_k$, and the collocation points, $\bar{x}_j$, $\bar{y}_l$,

are defined as the roots of the Jacobi polynomials as follows:

$$P_N^{(\zeta-1,\zeta-1)}(\bar{s}_i) = 0;\ P_{N-1}^{(\zeta,\zeta)}(\bar{x}_j) = 0; \tag{6.9}$$

$$P_N^{(\zeta-1,\eta-1)}(\bar{t}_k) = 0;\ P_{N-1}^{(\zeta,\eta)}(\bar{y}_l) = 0. \tag{6.10}$$

The corresponding weights are obtained from the Gauss-Jacobi integration formula (see [10]).

Note that since the subsidiary conditions which impose kinematic restrictions on all problems require integrations to be performed along y = 0 and x = 0, additional integration points and weights are needed. The integration points appropriate to the interval (0,c) along y=0 are obtained from

$$P_N^{(\eta-1,0)}(\bar{x}_i) = 0, \tag{6.11}$$

while the ones for (0,h) along x = 0 are obtained from the Legendre polynomials, as the Gauss formula for numerical integration may be used in this case, since there are no singularities at the end points of the interval. The zeros of the Legendre polynomials (integration points), and the weights associated with the Gauss formula can be obtained from several sources (see e.g. Abramowitz and Stegun [11]).

The corner conditions are in the forms given by Eqs. (3.16)-(3.17), where, for the cases of vertical and horizontal translation, the following relationships are valid:

$$A_0 = \bar{A}(1)/2^{\eta}\gamma^{\zeta},\ B_0 = \bar{B}(1)/2^{\eta}\gamma^{\zeta};$$
$$A_0' = \bar{A}(-1)/2^{\eta}\gamma^{\zeta},\ B_0' = \bar{B}(-1)/2^{\eta}\gamma^{\zeta}; \tag{6.12}$$

$$C_0, D_0, E_0, F_0 = \bar{C}(1),\ \bar{D}(1),\ \bar{E}(1),\ \bar{F}(1). \tag{6.13}$$

For the rotation of the rigid block problem Eq. (6.12) is replaced by:

$$A_0 = 2^{1-\eta_\gamma 2-\zeta_{\bar{A}}(1)},\ B_0 = 2^{1-\eta_\gamma 2-\zeta_{\bar{B}}(1)};$$
$$A_0' = 2^{1-\eta_\gamma 2-\zeta_{\bar{A}}(-1)},\ B_0' = 2^{1-\eta_\gamma 2-\zeta_{\bar{B}}(-1)}. \tag{6.14}$$

The barred quantities in Eqs. (6.12)-(6.14) have already been defined.

The procedure for obtaining solutions is the same for all three types of loading applied to the rigid block, and is as follows. The symmetries of A(s) and B(s) are used to collapse the parts of the normalized equations containing them, thereby eliminating N of the unknown quantities. The problem is thus reduced to finding the solution to a system of 3N simultaneous algebraic equations in the 3N unknowns $\bar{A}(\bar{s}_i)$, $\bar{B}(\bar{s}_i)$, $\bar{C}(\bar{t}_k)$, and $\bar{D}(\bar{t}_k)$, where i = 1,2,...,N/2, and k = 1,2,...,N. The governing singular integral equations provide 3N-4 equations, and the subsidiary conditions supply four more for a total of 3N. It is also noted that in Eqs. (3.30), (4.12), and (5.11) the unknowns are expressed as polynomials with N/2 terms by the use of Lagrange's interpolation formula (see e.g. Davis [12]).

Similarly, the two-inclusion problems formulated in chapters III-V lead to sets of 2N algebraic equations which are solved for the non-dimensionalized quantities $\bar{C}(\bar{t}_k)$ and $\bar{D}(\bar{t}_k)$, where k = 1,2,...,N.

RESULTS AND DISCUSSION

The numerical analysis was completed for a range of the geometric parameter γ ($0.05 \leq \gamma \leq 8$), and for Poisson's ratio (plane strain) of $\nu = 0.3$. The rate of convergence was tested by varying the number of points used at eight point intervals, from N = 16 to N = 48. The convergence of the global results appeared satisfactory and will be discussed in detail later. All results presented in this dissertation will be given for N = 48.

The results for the respective problems of vertical displacement, horizontal translation without rotation, and rotation of an embedded rectangular block will be given next.

Vertical displacement. The load diffusion curves for several values of γ are shown in Fig. 4 for the case when the block moves vertically without rotation. The load acting on the block at a distance y below the surface is given as a fraction of the total load, where both load and distance have been put in dimensionless form. The load given by the intersection of the load-diffusion curves and the $y = h$ axis represents the load carried by the base of the block for each γ. Analogous to the block problem is that of two parallel inclusions, each subjected to a vertical load P and having no rotation. The results for this problem can be compared with those of the vertical displacement for the block. The load diffusion, calculated for the two-inclusion case, is shown in Fig. 5, where it is compared to the rigid block results; the solid lines represent values obtained from Fig. 4, and the dashed lines represent the two-inclusion case. These

latter curves go to zero at $y = h$, since there is no base to carry part of the load. Furthermore, the dashed and solid curves are relatively close provided that $0 < y < 0.8h$. Thus, for relatively slender blocks, a solution which ignored the base would give approximately valid results. Figure 6 shows the percentage of the applied load P carried by the side of the rectangular block as a function of c/h. As expected, when c/h is small most of the load is carried by the sides; as c/h increases the base carries a larger share of the load. When γ is approximately equal to 0.42, the sides and the base each carry half the load.

Figures 7 and 8 show the variations, respectively, of the discontinuities in the normal stresses along the base of the block, and those in the shear stresses along the sides for several values of c/h. Since a zero stress state prevails throughout the rigid block, these stress discontinuities represent the <u>actual</u> stress distributions along the walls of the elastic body surrounding the block, as is evident from the definitions of $A(x)$, $B(x)$, $C(y)$, and $D(y)$. Also, since the normal stresses are symmetric along the base, they are plotted only for $0 < x < c$ and exhibit singular behavior at the end $x = c$. The shear stresses are plotted for $0 < y < h$, and singular behavior is noted near both ends, $y = 0,h$. It is further observed that the magnitudes of both $A(x)$ and $D(y)$ vary proportionately with the amount of load carried by the base and the sides, respectively. Thus, the magnitude of $A(x)$ increases with γ, while the magnitude of $D(y)$ decreases as γ increases.

One estimate of the accuracy of the results may be obtained by calculating the displacements in the y-direction along the surface of

the block y = 0, relative to the midpoint (0,0). Since the block translates as a rigid body along y, these displacements should be small when compared to those obtained from the solution of the two-inclusion problem undergoing vertical displacement. The results of this comparison are given in Table 1. It is noted that the displacements at the corner x = c for the two inclusion problem vary from being approximately 18 times greater than the block displacements (for $\gamma = 0.3$), to being 175 times greater (for $\gamma = 4$). The displacements obtained for the rigid block problem tended to oscillate about zero, while the ones for the two inclusion problem grew with distance from (0,0), as expected. It should be added that for $\gamma < 0.3$, the value of the ratio $|u_{y_b}/u_{y_2}|$ approaches unity. That is, as the block becomes slender, the presence (or absence) of the base has little or no effect on the results calculated near the surface. Therefore, a comparison of those results for the purposes of Table 1 would have little meaning, since the surface displacements are already small to within the accuracy of the solution.

Horizontal displacement without rotation. Figures 9-12 present results obtained from the solution of the embedded block undergoing horizontal displacement. Figure 9 shows the variation with γ of the percentage of the total load that is carried by the side of the rigid block. In this case, the point at which half of the load is carried by the sides and half by the base is approximately $\gamma = 1.5$.

The shear stress distribution along the base of the block, and the normal stress distribution along the side x = c of the block are shown for several values of γ in Figs. 10 and 11, respectively. The results showing the variation of the magnitudes of the stresses with

γ are analogous to the results for the vertical displacement case; the magnitude of the stresses tends to increase with the amount of load carried by the surface of the block upon which they act.

Since the block translates horizontally without rotation, an applied moment, M, in addition to a horizontal load, 2Q, must be applied to prevent the block from rotating. The ratio M/Qh is plotted in Fig. 12 as a function of c/h. At the limit, as c/h approaches zero, the results are in agreement with the result obtained from the solution for a single inclusion perpendicular to the free surface, y = 0, and loaded by a horizontal force, 2Q, and a moment, M, such that the inclusion translates in the negative x-direction without rotation.

Rotation. Results obtained for the problem of rotation of the embedded rigid block are presented in Figs. 13-17. The normal and shear stresses acting on the base of the block are given in Figs. 13-14 as functions of the distance from the midpoint, for several values of c/h. The normal and shear stress distributions along the sides of the block for $0 < y < h$, are plotted, respectively, in Figs. 15-16. The curves show the variation of the magnitude and sign of the stresses with γ. A better understanding of the mechanics of the problem can be obtained by examining the moment equilibrium equation for the block, which is given next:

$$M = -\int_{-c}^{c} A(x)x\,dx + h\int_{-c}^{c} B(x)\,dx + 2\int_{0}^{h} C(y)y\,dy$$
$$-2c\int_{0}^{h} D(y)\,dy. \qquad (6.15)$$

In writing Eq. (6.15) use has been made of Eq. (5.3). Using the symmetries of A(x) and B(x) appropriate for the rotation problem, and

incorporating Eqs. (6.1)-(6.2), and (6.5)-(6.6), Eq. (6.15) is written in the normalized form given next:

$$\frac{1}{\mu h^2}\frac{M}{\alpha} = \frac{\pi(\kappa+1)}{\kappa}\left[-4\gamma^3\int_0^1 \bar{A}(\bar{x})\,\bar{x}\,(1-\bar{x}^2)^{\zeta-1}d\bar{x}\right.$$
$$+ 4\gamma^2\int_0^1 \bar{B}(\bar{x})\,(1-\bar{x}^2)^{\zeta-1}d\bar{x}$$
$$+\int_{-1}^1 \bar{C}(\bar{y})\,(1+\bar{y})\,(1-\bar{y})^{\zeta-1}(1+\bar{y})^{\eta-1}d\bar{y}$$
$$\left.-2\gamma\int_{-1}^1 \bar{D}(\bar{y})\,(1-\bar{y})^{\zeta-1}(1+\bar{y})^{\eta-1}\,d\bar{y}\right]. \qquad (6.16)$$

Equation (6.16) may be written as

$$\frac{1}{\mu h^2}\frac{M}{\alpha} = A_S + B_S + C_S + D_S, \qquad (6.17)$$

where the definitions of the quantities A_S, ..., D_S are readily obtained by comparing Eqs. (6.16) and (6.17). The ratio $M/\mu h^2\alpha$ represents a measure of the rotational stiffness of the partially embedded rigid block. Therefore, the quantities A_S, B_S, C_S, and D_S represent the contribution made to the stiffness by the stresses $A(x)$, $B(x)$, $C(y)$, and $D(y)$, respectively. Table 2 shows the variation of these quantities with γ. Note that the contribution of the normal stresses acting on the base of the block becomes significant only for $\gamma \geq 1$, while the opposite is true for the normal stresses acting on the sides (their contribution becomes more important as γ becomes smaller). It is also observed that the contribution of the base shear stresses to the total stiffness remains proportionately low for all values of γ, while that of the side shear stresses increases with γ.

By dividing $M/\mu h^2\alpha$ by γ^2, one obtains a new ratio, namely $M/\mu c^2\alpha$. These two ratios are plotted as functions of γ in Fig. 17. There are

two limiting tests for these results: 1) as c/h tends to zero, the results for $M/\mu h^2\alpha$ tend to the single inclusion result; 2) as c/h becomes large the results may be compared to the one obtained by Muskhelishvili for the rotation of a rigid stamp bonded to an elastic body (see [13], p. 492, Eq. 114.19a). As may be seen in Fig. 17, the two limiting cases seem to support the accuracy of the calculated results.

The corner conditions derived for the corner (c,h) were checked by calculating the values of the stress discontinuities at that corner, and substituting in Eqs. (3.16). The corner values were calculated by a quadratic extrapolation applied to the three points nearest that corner. It was found that the corner conditions were not satisfied; the size of the error was generally of the same order of magnitude as some of the individual terms. Even though an allowance must be made for the error introduced by the quadratic extrapolation, this size error is still considered large for the present type of analysis. To correct this discrepancy, and more importantly, to check the accuracy of the global results, three of the corner conditions given in Eqs. (3.16) were incorporated in the system of 3N equations, by removing the equations closest to the corner (c,h) from the corresponding boundary conditions. This new system of equations yielded results which, away from the corner (c,h) matched the results previously obtained very closely (to four significant figures), and in addition, satisfied all the corner conditions. Moreover, the global results obtained using this new system of equations varied slightly from the ones obtained previously, as it will be shown later. To further test the sensitivity of the global results to the collocation

scheme used, the order of the singularity at (c,h) was changed from $\zeta - 1 = -0.40484$ to -0.5, and the calculations were repeated with N = 48. Lastly, the singularities at (c,h) and (c,0) were set equal to -0.5, and a new set of results obtained for N = 48. A comparison of some of the results obtained from these solutions is given in Tables 3-4. An examination of these tables shows that the global results remain relatively unaffected by small changes in the order of the corner singularities.

It should be noted that when the order of the singularities at both (c,h) and (c,0) was taken as -0.5, the related Jacobi polynomials reduced to the Chebyshev polynomials of the first kind (see e.g. [11]). Numerical solutions of Cauchy-type singular integral equations with regular kernels obtained by use of the Gauss-Chebyshev integration formula, have been shown to converge to the correct results by Erdogan and Gupta [14], and Kalandiya [15]. Furthermore, Kalandiya states in [15] that this method was also successfully applied to problems with generalized kernels. Of course, as the singularities used here are not of the correct order, this method cannot be expected to yield correct results at the corners. However, the fact that the global results obtained by use of the Gauss-Chebyshev integration formula match closely those obtained using the Gauss-Jacobi integration formula, as may be seen in Tables 3-4, is supportive of the validity of the global results.

Although the accuracy of the global results obtained by use of the collocation scheme introduced in [8] has been shown to be satisfactory, the accuracy of the results in the vicinity of the corners is not certain. There are two reasons for this: 1) A second root is

present at the corner (c,h) and is not taken into account; this root has a singular contribution of order 0.75904-1 = -0.24096 near that corner. As pointed out by Westmann in [7], although the stress field in the vicinity of the corner is dominated by the largest singularity, the presence of two singular terms may be important to the problem.

2) In two recent papers, [16, 17], Theocaris and Ioakimidis suggest that the collocation points as determined for the Gauss-Jacobi method may not be the correct ones. In [16], it is suggested that the rate of convergence of the results can be improved by a different choice of collocation points associated with the Gauss-Jacobi integration rule, or by using a different scheme such as the Lobatto rule. The collocation points for the case of real singularities are, respectively, the roots of the Jacobi-functions, and of their derivatives (see Elliot [18]). In [17], the problem of an antiplane shear crack terminating at a bimaterial interface solved by Erdogan and Cook [19], was reconsidered, and numerical results were obtained by using the modified Gauss-Jacobi and the Lobatto-Jacobi methods discussed in [16]. It was found that while in general the results of [17] matched closely those of [19], the value of the stress intensity factor at the interface obtained by Theocaris and Ioakimidis was in much better agreement with the theoretical result than that obtained by Erdogan and Cook. However, the rate of convergence was not satisfactory. The authors attributed this to the existence of a second singularity of positive order near the interface. A technique is proposed for accounting for both singularities in the analysis, and this results in a much faster convergence of the results to the theoretical value. However, it should be realized that this technique could not be applied to the

present analysis, since it deals with singularities of opposite signs.

In view of the arguments just presented, the accuracy of the corner values of the stress discontinuities obtained in the present analysis, by use of the collocation scheme introduced in [8], is uncertain. However, for completeness, a discussion of these values is presented in Appendix B.

To investigate the rate of convergence of the global results, the number of points taken was varied at eight point intervals, from N=16 to N=48. Several of the calculated global results are presented in Tables 5-7. Tables 5-6 show the calculated values for the portion of the load carried by the sides of the block for the vertical and horizontal displacement cases, respectively. The variation of the ratio $M/\mu h^2\alpha$ with N, is shown for several values of c/h in Table 7. It is seen that the rate of convergence of these representative global quantities is quite satisfactory.

CHAPTER VII

CONCLUSIONS

The formulation of the boundary value problem of a rigid rectangular block partially embedded in, and perfectly bonded to an elastic half space led to a system of singular integral equations, whose unknowns were the discontinuities in the stresses between the bonded surfaces. Three separate loading conditions were applied causing the block to 1) translate vertically without rotation, 2) translate horizontally without rotation, and 3) rotate about an axis in the z-direction.

A numerical solution for the systems of equations governing each problem was obtained by using the collocation scheme introduced by Erdogan, Gupta, and Cook. Results were computed for several values of the geometric parameter $\gamma = c/h$.

The accuracy of the results was checked in several ways, and it proved quite satisfactory for global quantities such as:

1) Load diffusion from the block into the elastic half space (vertical displacement problem);
2) Percentage of load carried by the sides and the base of the block (vertical and horizontal displacement problems);
3) Ratio of applied moment to horizontal load (horizontal displacement problem);
4) Moment stiffness (rotation problem);
5) Normal and shear stress distribution along the sides and base of the block, excluding the vicinity of the corners $(\pm c, h)$ (all problems).

Since the corner conditions and the singular behavior near the corners ($\pm c, h$) were not satisfied, local qualities such as the shear and normal stresses are only valid away from these corners.

x/c \ c/h	$\lvert u_{y_b}/u_{y_2} \rvert$				
	0.3	0.5	1	2	4
0.2	0.3092	0.0547	0.0018	0.0028	0.0016
0.4	0.0154	0.0119	0.0101	0.0011	0.0010
0.6	0.2421	0.0461	0.0051	0.0002	0.0007
0.8	0.0258	0.0132	0.0092	0.0047	0.0015
1	0.0544	0.0178	0.0149	0.0081	0.0057

TABLE 1 Vertical Displacement: *Comparison of the y-displacements* relative to the midpoint at the surface y = 0 of the rigid block (u_{y_b}) and the two-inclusion (u_{y_2}) problems for several values of $\gamma = c/h$.

c/h	A_S	B_S	C_S	D_S
0.05	-0.002	-0.236	1.232	-0.061
0.1	-0.006	-0.505	1.550	0.147
0.2	-0.020	-1.026	2.115	0.372
0.3	-0.036	-1.568	2.739	0.664
0.5	0.002	-2.091	3.350	1.356
1	1.123	-0.083	1.738	2.913
2	6.424	2.680	-0.255	6.656
4	27.685	4.369	-0.959	18.175

TABLE 2 Rotation: Variation of the contributions of the stresses to the rotational stiffness of the embedded block with γ.

CASE / c/h	Portion of applied load carried by the sides of block							
	0.05	0.1	0.2	0.3	0.5	1	2	4
1	0.7797	0.7079	0.6026	0.5349	0.4606	0.3658	0.2704	0.1927
2	0.7850	0.7109	0.6090	0.5444	0.4708	0.3741	0.2789	0.2027
3	0.7835	0.7106	0.6015	0.5315	0.4555	0.3592	0.2627	0.1837
4	0.7839	0.7098	0.5961	0.5242	0.4500	0.3503	0.2638	0.1832

TABLE 3 Vertical Displacement: Comparison of the portion of applied load carried by the sides of the block, calculated by: 1) Using the correct singularities (ζ^{-1}, η^{-1}); 2) Using the correct singularities and three of the corner conditions; 3) Assuming square root singularity at (c,h); 4) Assuming square root singularity at both (c,h) and (c,0).

CASE / c/h	Vertical displacement of corner (c,0) relative to (0,0)							
	0.05	0.1	0.2	0.3	0.5	1	2	4
1	0.00191	0.00253	0.00197	0.00102	0.00115	0.00231	0.00255	0.00270
2	0.00191	0.00253	0.00197	0.00102	0.00115	0.00231	0.00255	0.00270
3	0.00192	0.00256	0.00203	0.00110	0.00124	0.00237	0.00257	0.00271
4	0.00059	0.00139	0.00051	-0.00061	-0.00017	0.00191	0.00252	0.00270

TABLE 4 **Vertical Displacement:** Comparison of the error in the vertical displacement of the corner of the block (c,0) relative to (0,0) calculated by: 1) Using the correct singularities ($\zeta-1;\eta-1$); 2) Using the correct singularities and three of the corner conditions; 3) Assuming square root singularity at (c,h); 4) Assuming square root singularity at both (c,h) and (c,0).

N / c/h	Portion of Applied Load Carried by the Sides							
	0.05	0.1	0.2	0.3	0.5	1	2	4
16	0.1684	0.6641	0.5622	0.4689	0.4010	0.3357	0.2380	0.1565
24	0.6411	0.7000	0.5815	0.5016	0.4313	0.3498	0.2529	0.1752
32	0.7458	0.7052	0.5916	0.5183	0.4460	0.3574	0.2612	0.1835
40	0.7721	0.7069	0.5981	0.5283	0.4548	0.3623	0.2666	0.1889
48	0.7797	0.7079	0.6026	0.5349	0.4606	0.3658	0.2704	0.1927

TABLE 5 Vertical Displacement: Variation of the amount of load carried by the sides of the block with the number of points used, for several values of c/h.

N / c/h	Portion of Applied Load Carried by the Sides							
	0.05	0.1	0.2	0.3	0.5	1	2	4
16	0.8853	0.7597	0.7064	0.6905	0.6416	0.5338	0.4115	0.3031
24	0.8307	0.7448	0.6970	0.6795	0.6473	0.5554	0.4262	0.3149
32	0.8110	0.7390	0.6901	0.6730	0.6515	0.5677	0.4341	0.3227
40	0.8027	0.7351	0.6847	0.6687	0.6545	0.5759	0.4391	0.3276
48	0.7980	0.7317	0.6803	0.6654	0.6569	0.5819	0.4427	0.3311

TABLE 6 Horizontal Displacement: Variation of the amount of load carried by the sides of the block with the number of points used, for several values of c/h.

N / c/h	$M/\mu h^2\alpha$							
	0.05	0.1	0.2	0.3	0.5	1	2	4
16	1.0457	1.1898	1.4789	1.8050	2.6216	5.6960	15.5036	49.1522
24	1.0541	1.1880	1.4750	1.8028	2.6226	5.6964	15.5096	49.2397
32	1.0557	1.1868	1.4731	1.8013	2.6213	5.6944	15.5088	49.2604
40	1.0558	1.1861	1.4720	1.8001	2.6196	5.6922	15.5070	49.2674
48	1.0558	1.1856	1.4712	1.7991	2.6179	5.6903	15.5054	49.2699

TABLE 7 Rotation: Variation of the ratio $M/\mu h^2\alpha$ with number of points used, calculated for several values of c/h.

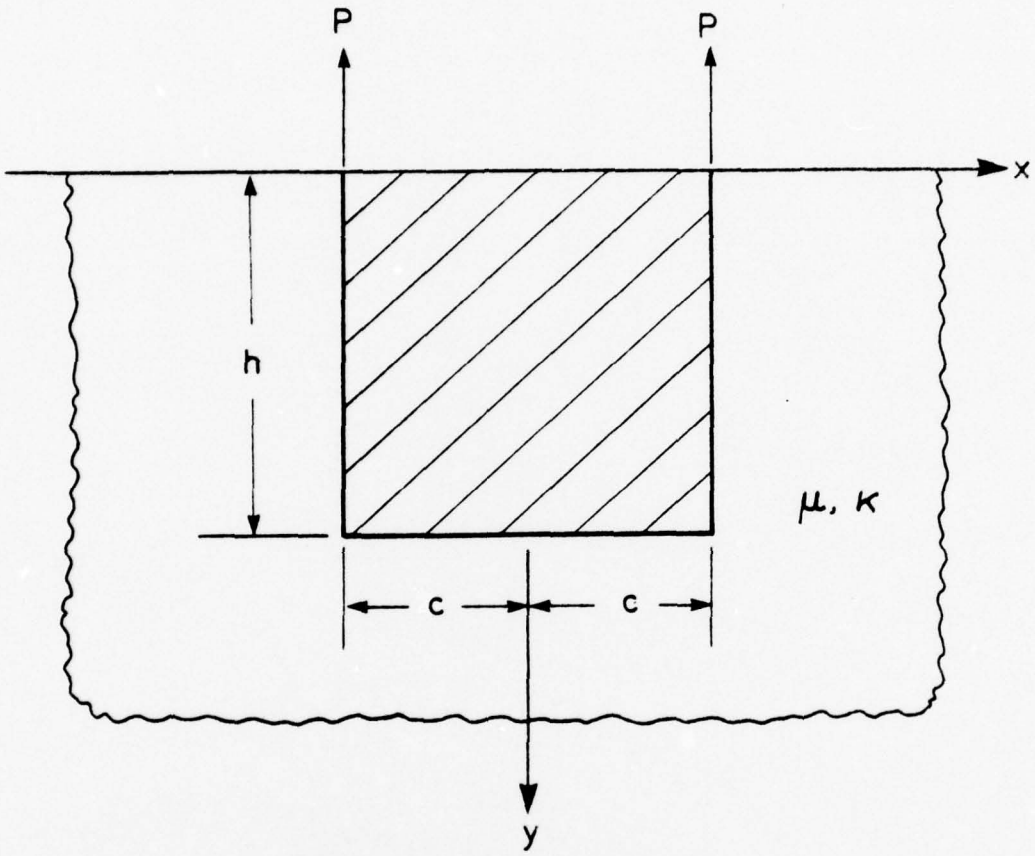

Fig. 1 Geometry and coordinate system for a partially embedded finite rigid block undergoing vertical translation.

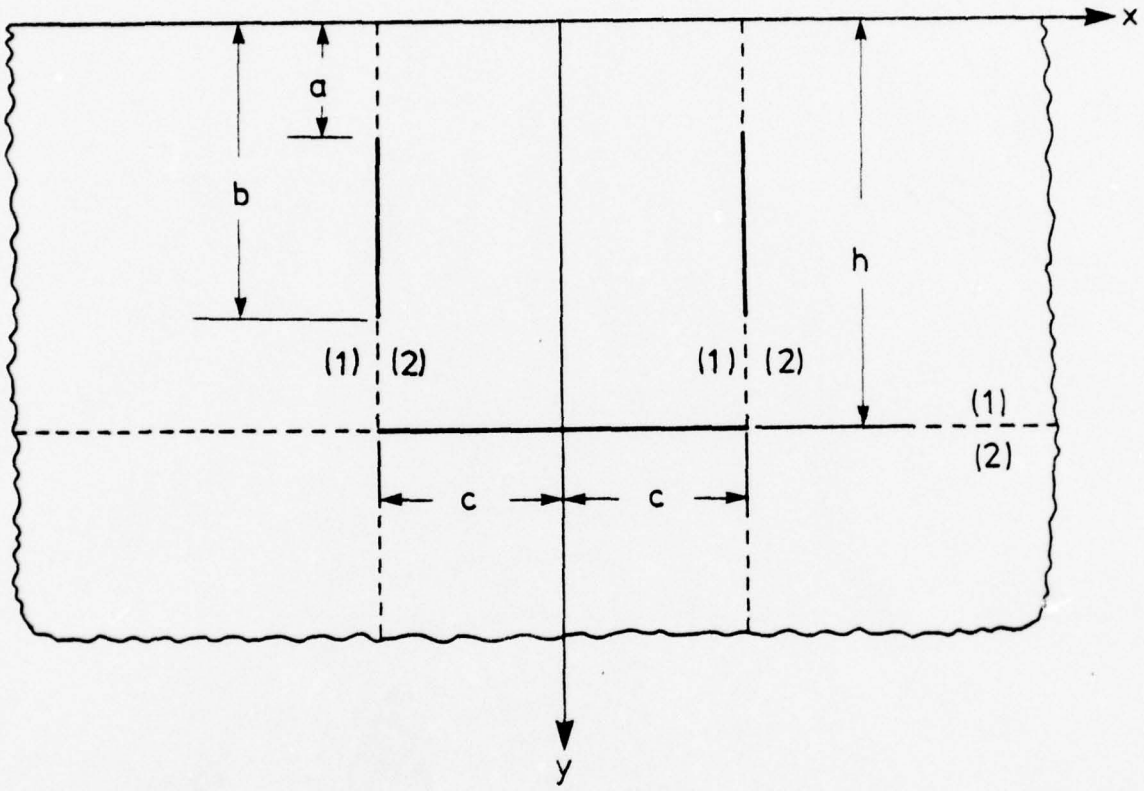

Fig. 2 Superposition solution.

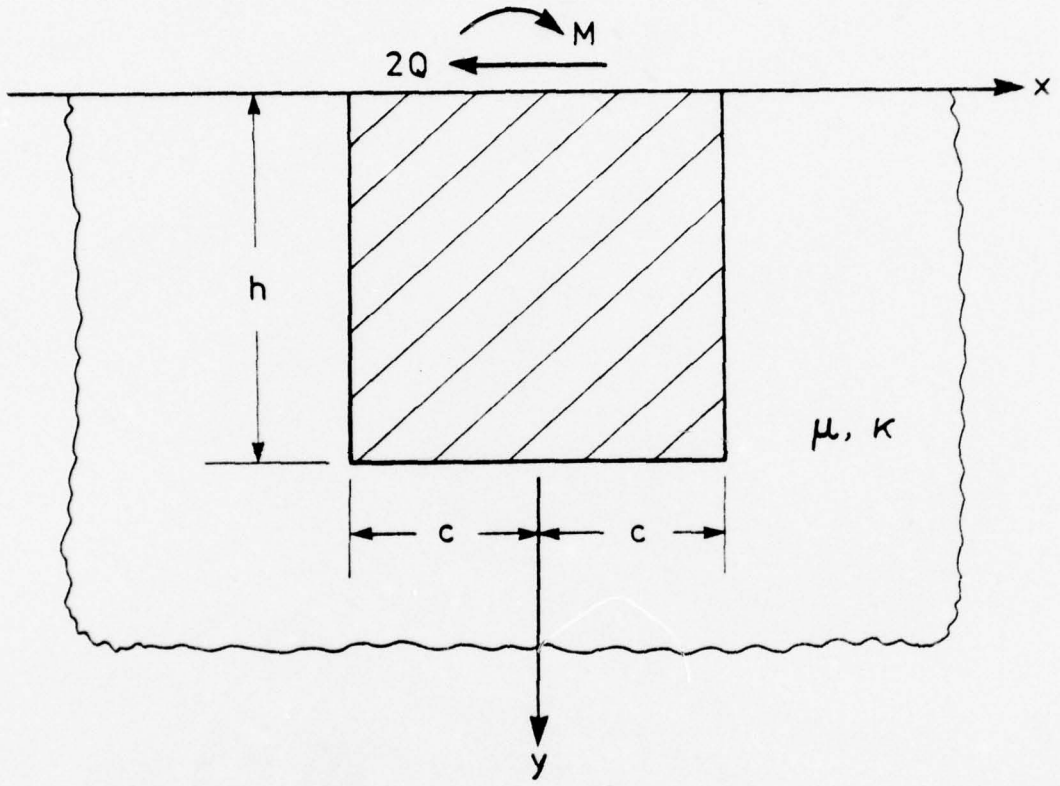

Fig. 3 Geometry and coordinate system for an embedded block undergoing horizontal translation without rotation.

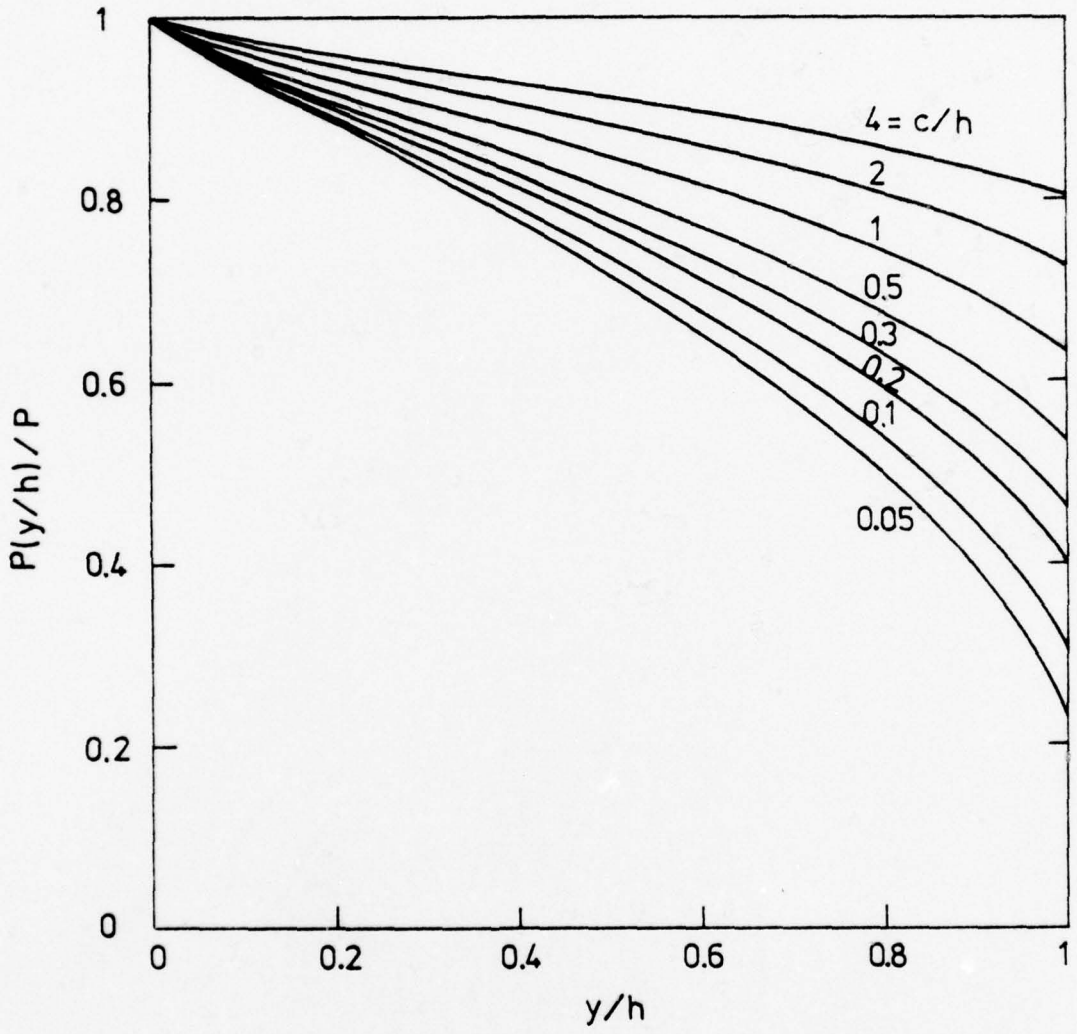

Fig. 4 Vertical Displacement: Load diffusion for various values of c/h.

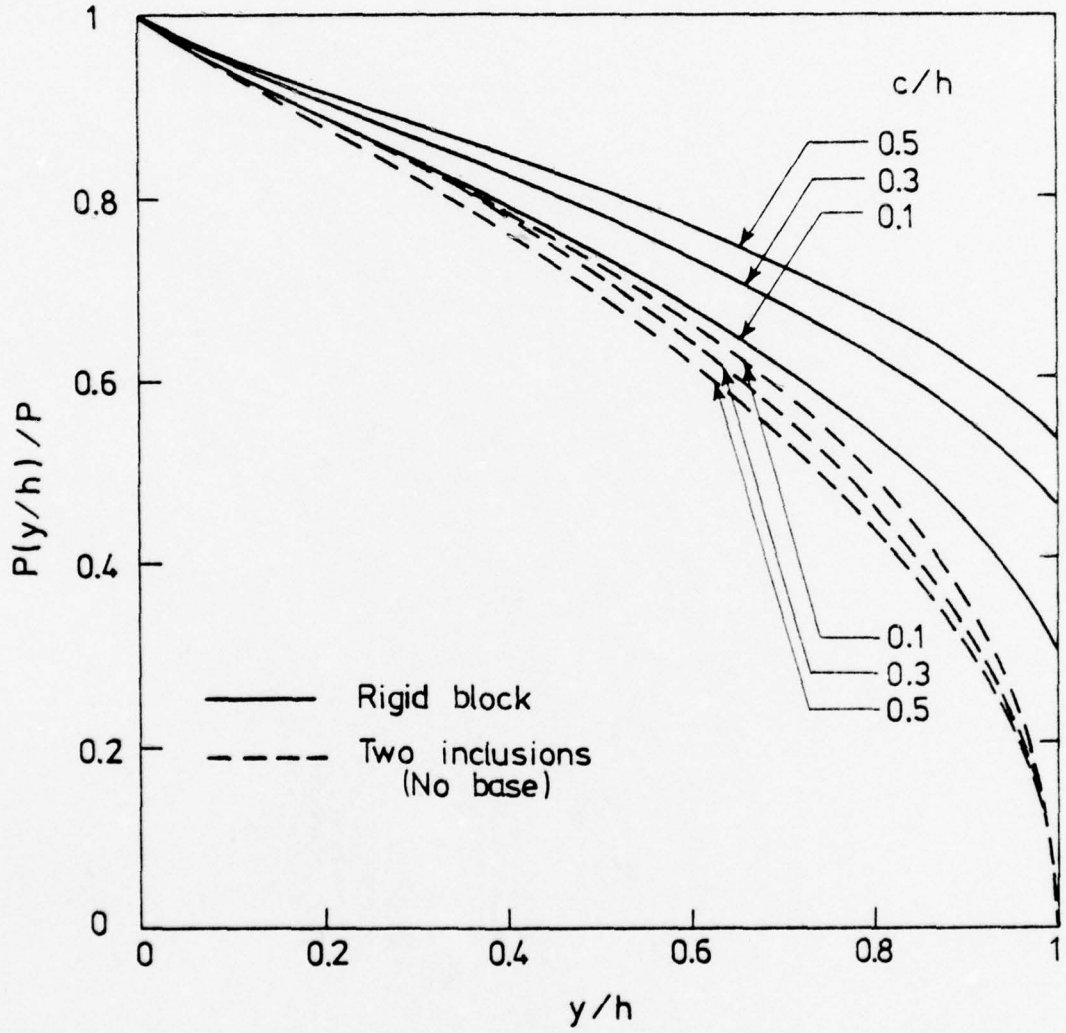

Fig. 5 Vertical Displacement: Comparison of load diffusion curves for the rigid block and the two-inclusion problems.

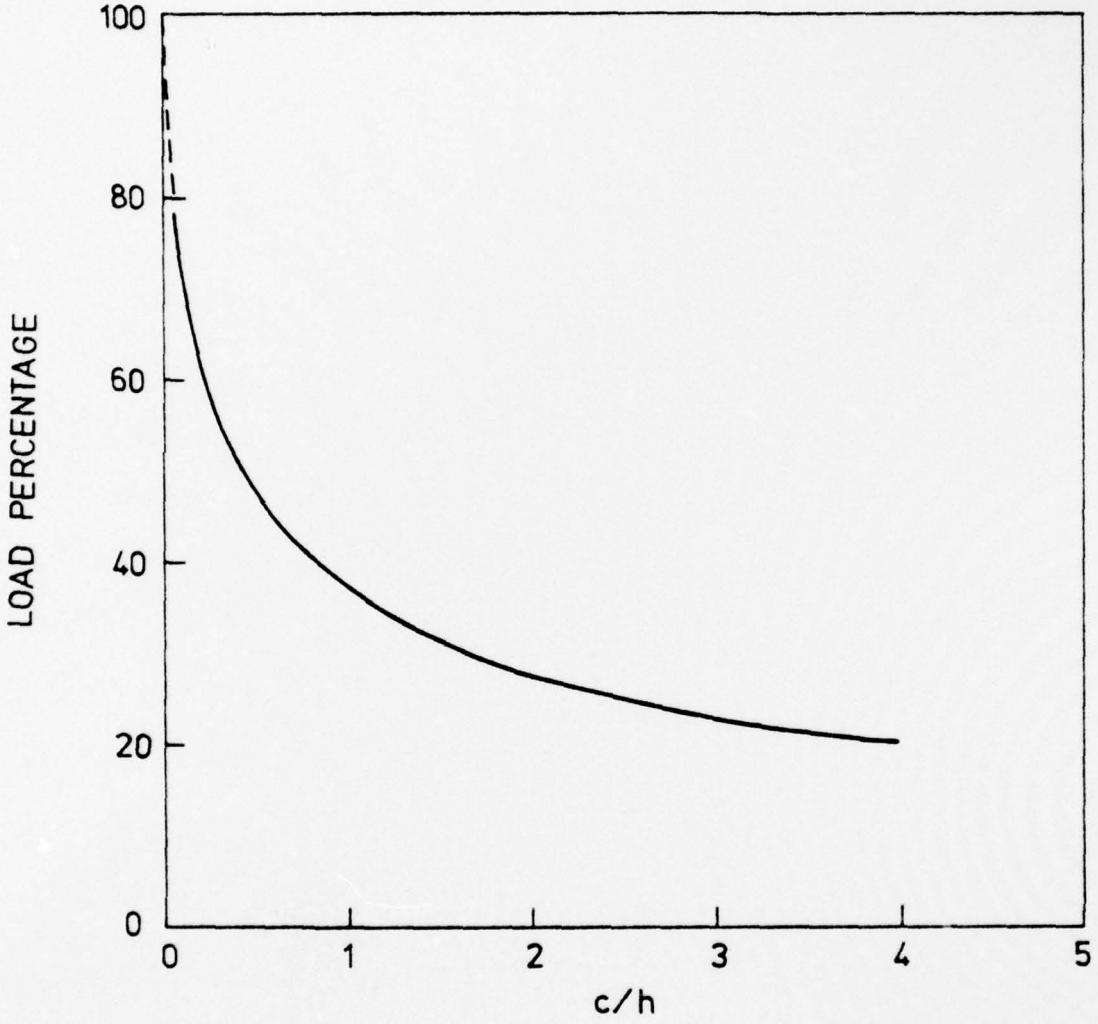

Fig. 6 Vertical Displacement: Percentage of the applied load P carried by each side of the rectangular block as a function of $\gamma = c/h$.

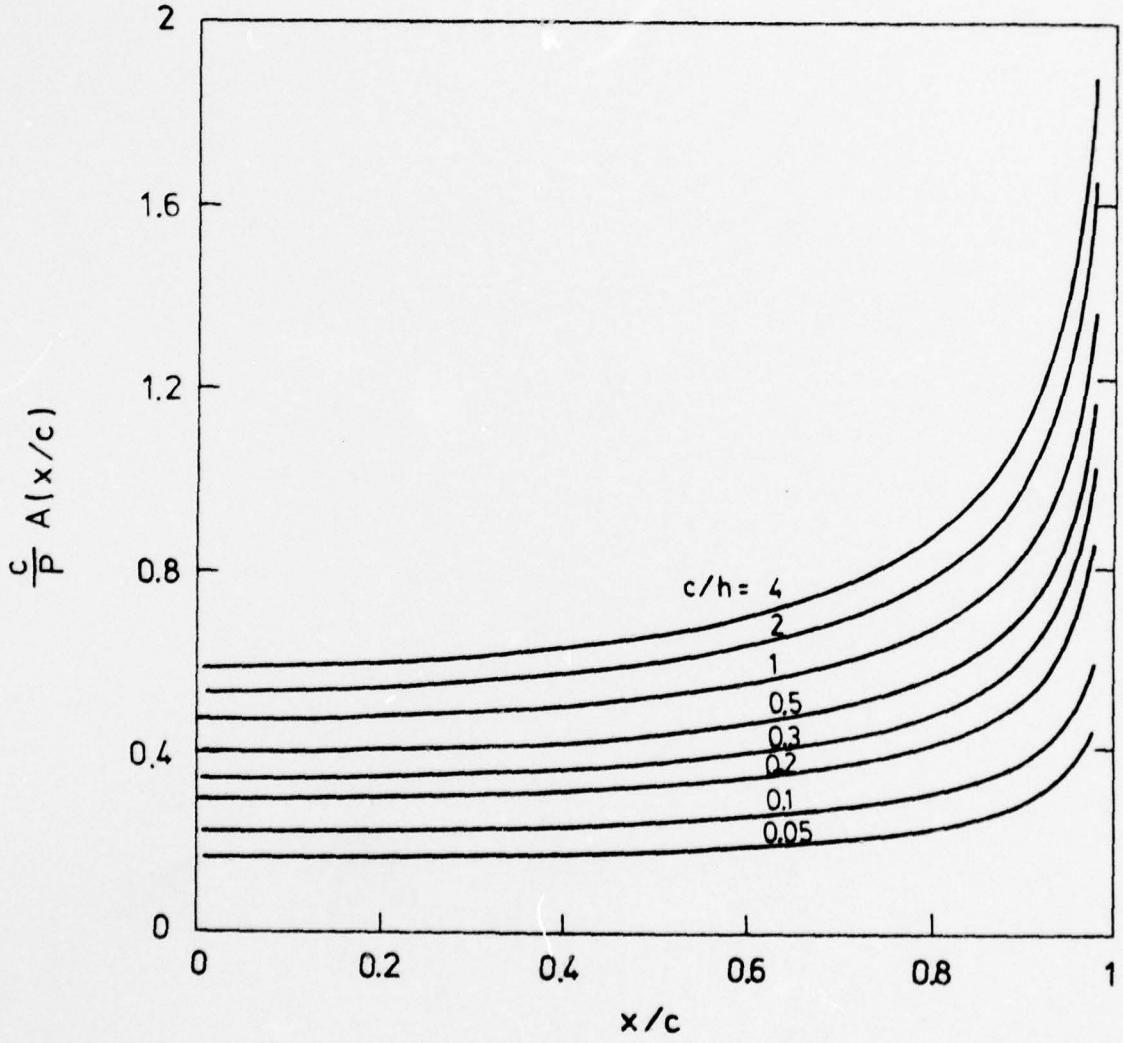

Fig. 7 Vertical Displacement: Normal stresses acting on base of block vs. distance from center for several values of c/h.

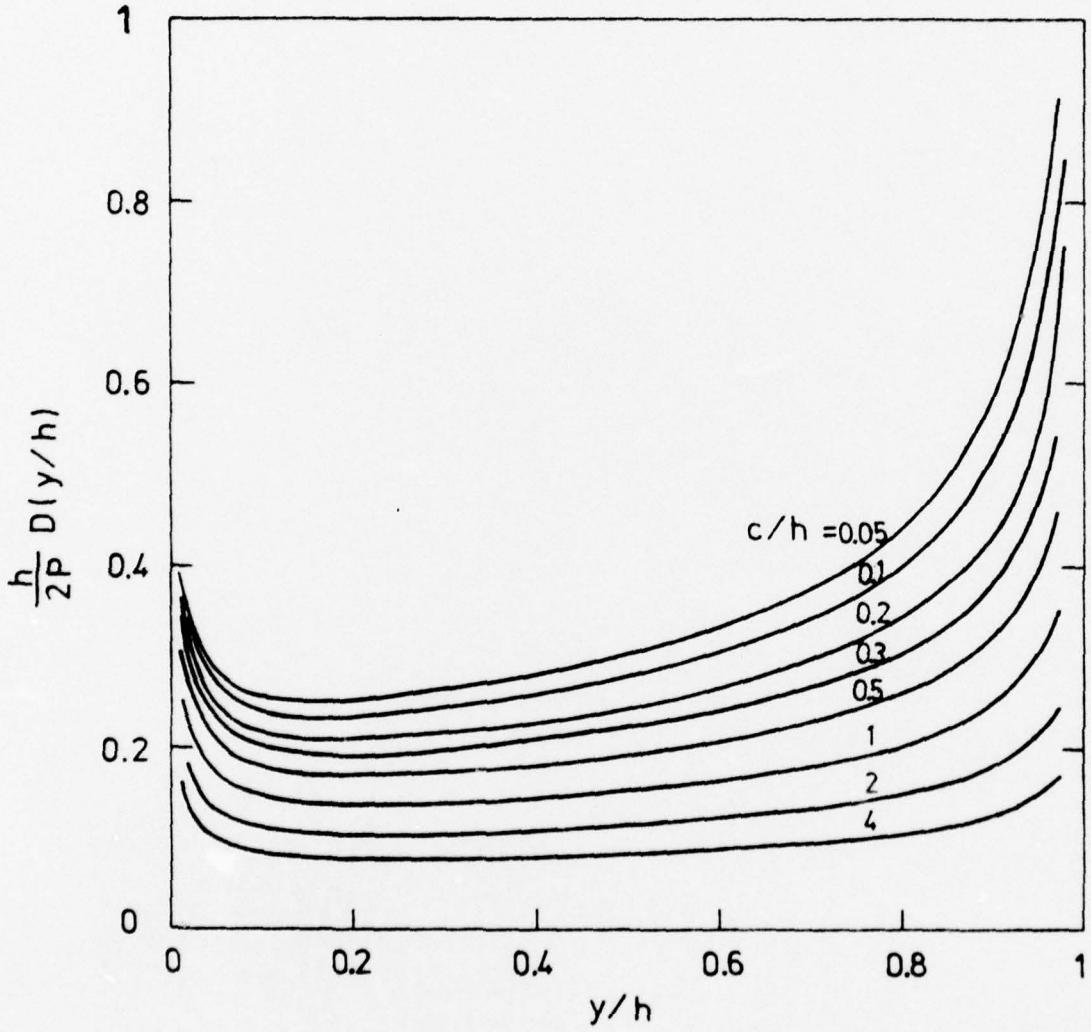

Fig. 8 Vertical Displacement: Shear stresses acting on side of block vs. distance from free surface for various values of c/h.

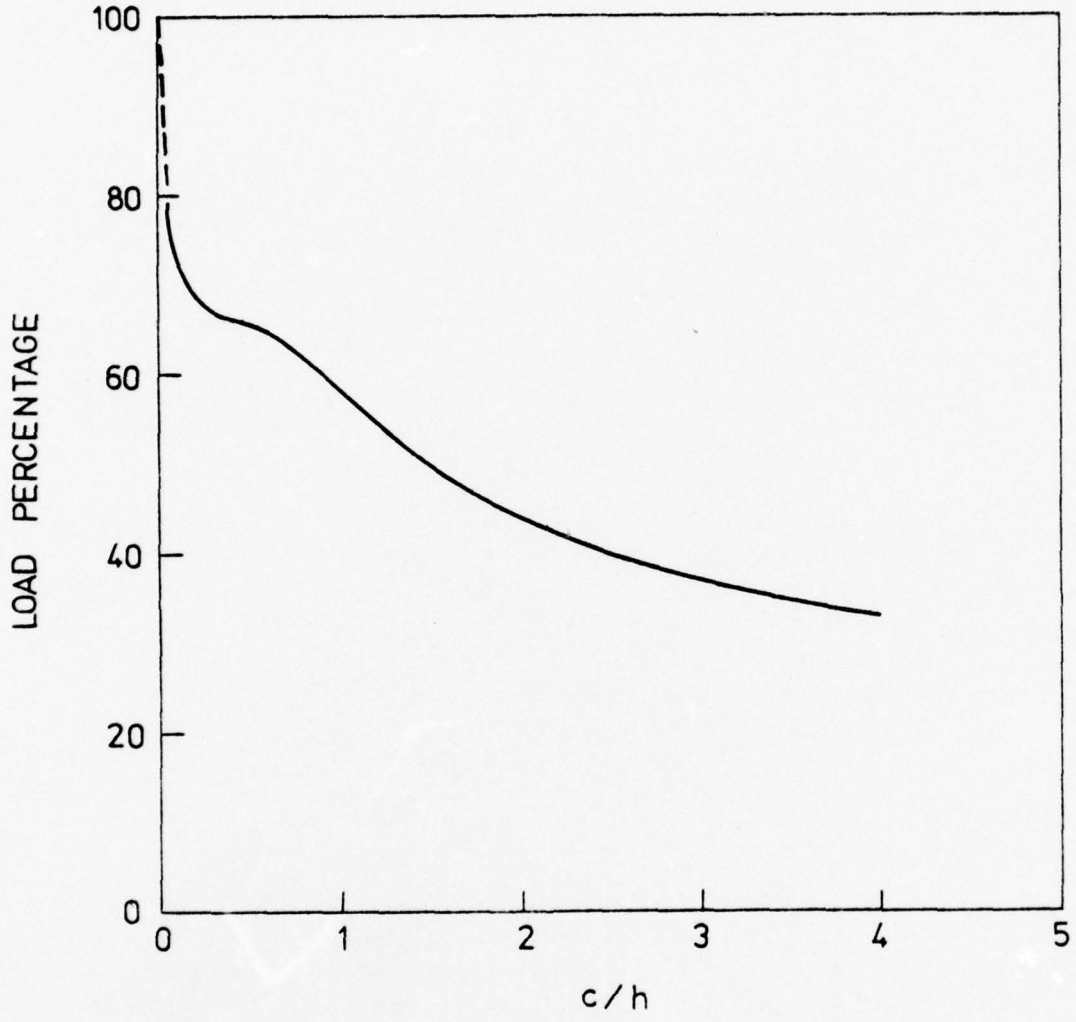

Fig. 9 Horizontal Displacement: Percentage of the applied shear load carried by the sides of the rigid block as a function of $\gamma = c/h$.

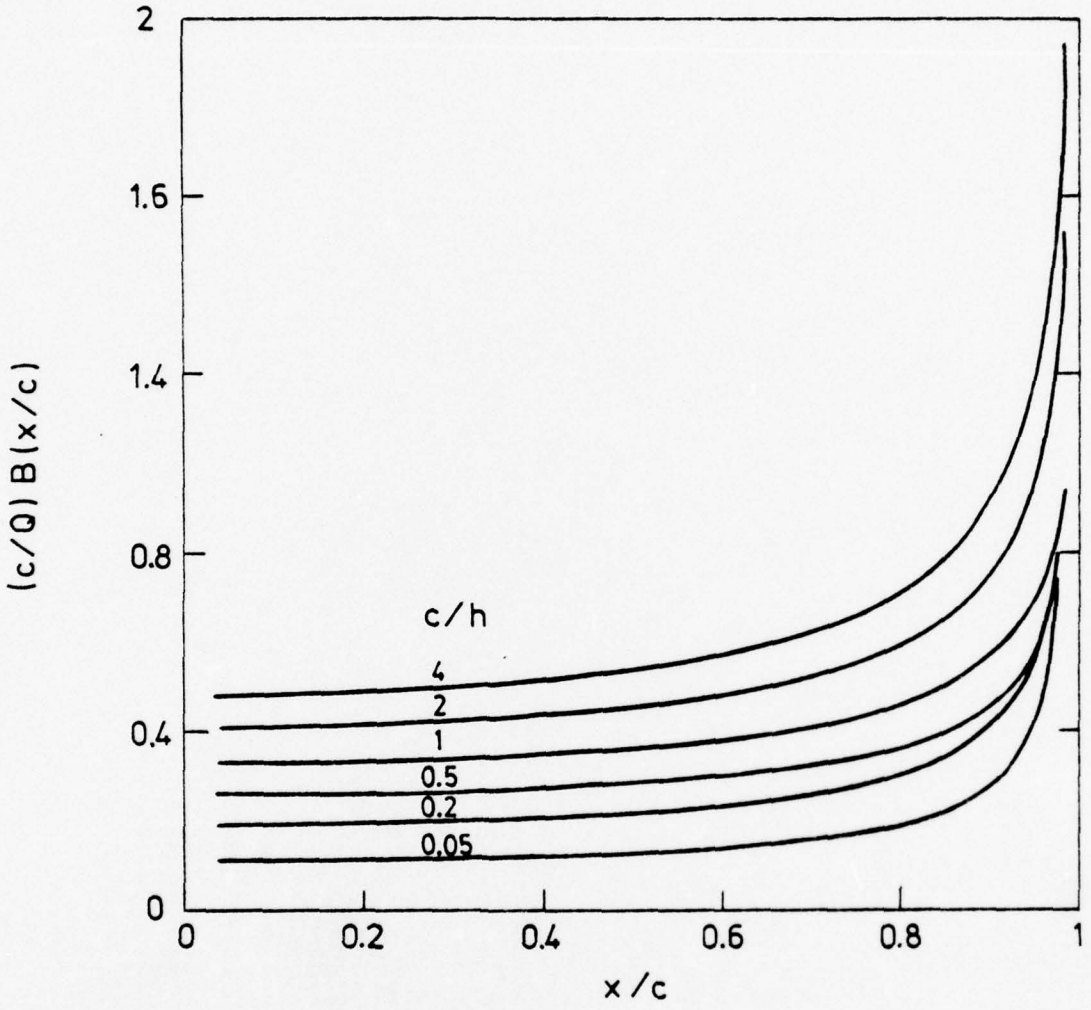

Fig. 10 Horizontal Displacement: Shear stress distribution along base of rigid block shown for $0 < x < c$ for several values of $\gamma = c/h$.

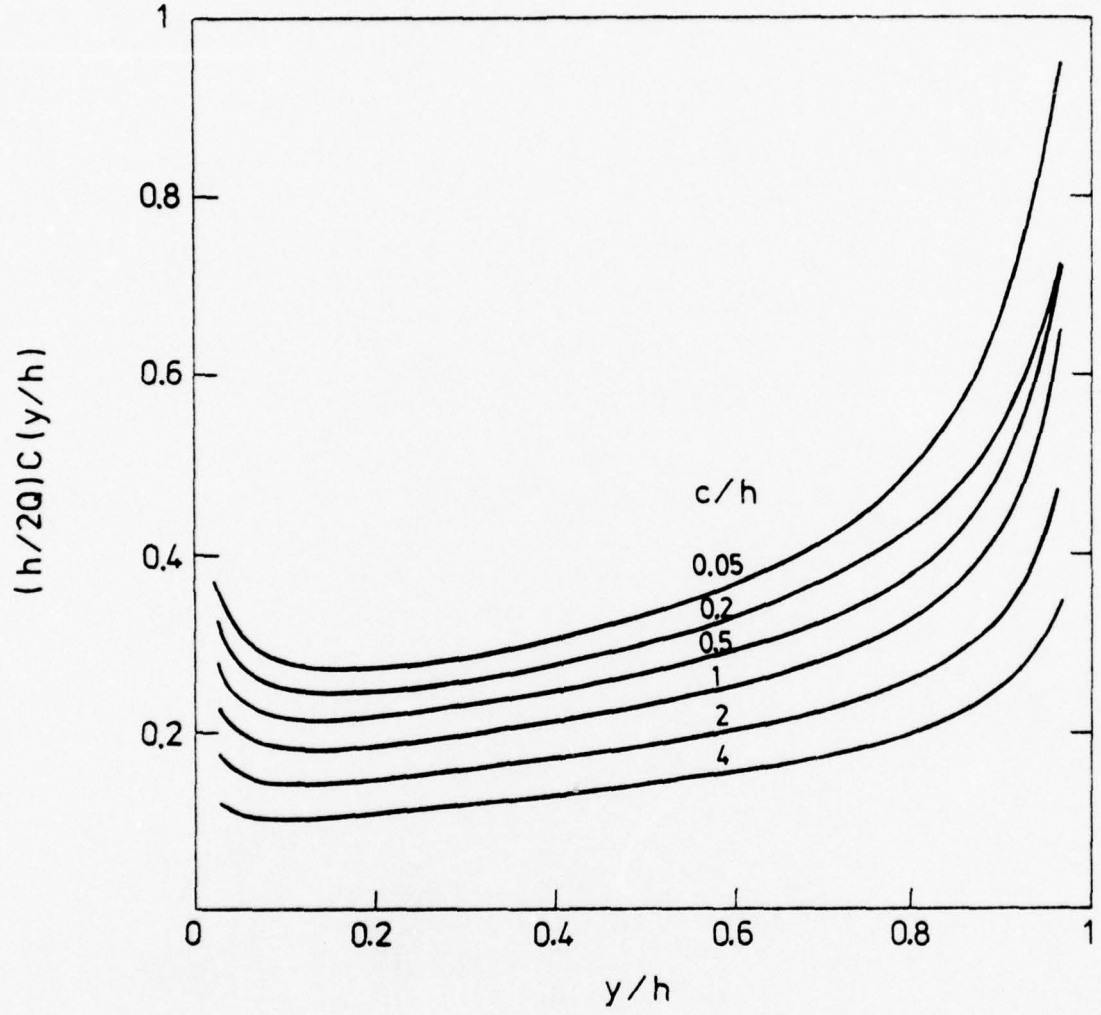

Fig. 11 Horizontal Displacement: Normal stress distribution along side of block ($0 < y < h$) for several values of $\gamma = c/h$.

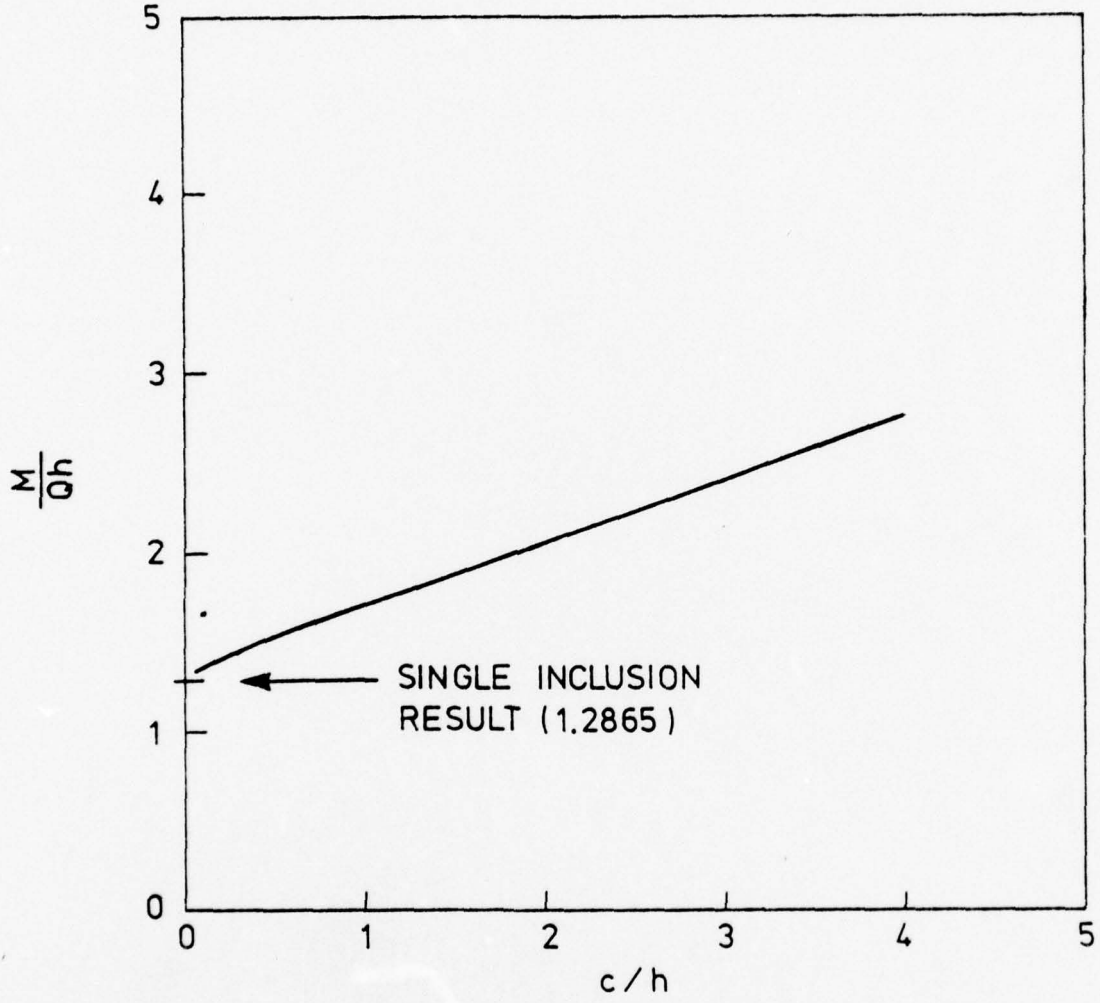

Fig. 12 Horizontal Displacement: The ratio M/Qh as a function of $\gamma = c/h$.

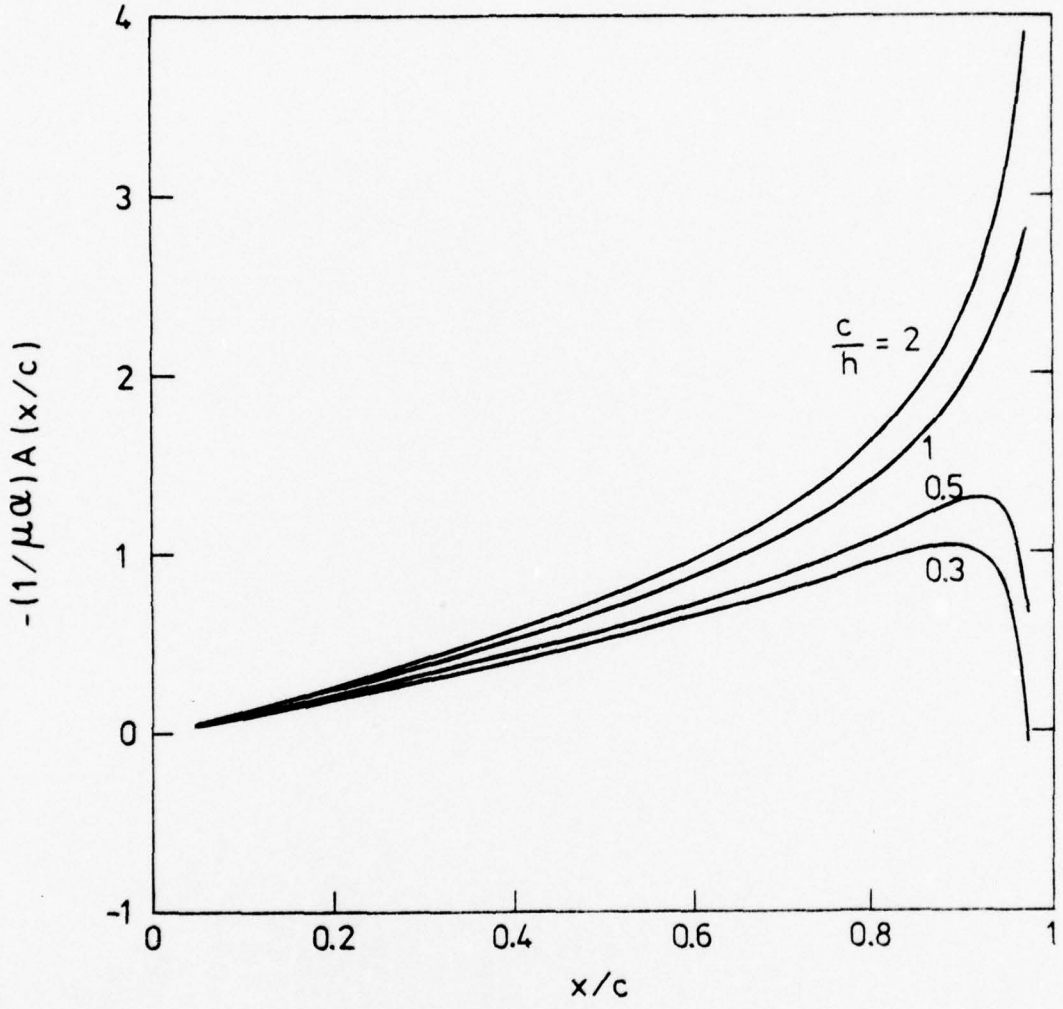

Fig. 13 Rotation: Normal stress distribution at y = h, 0 < x < c, for various values of c/h.

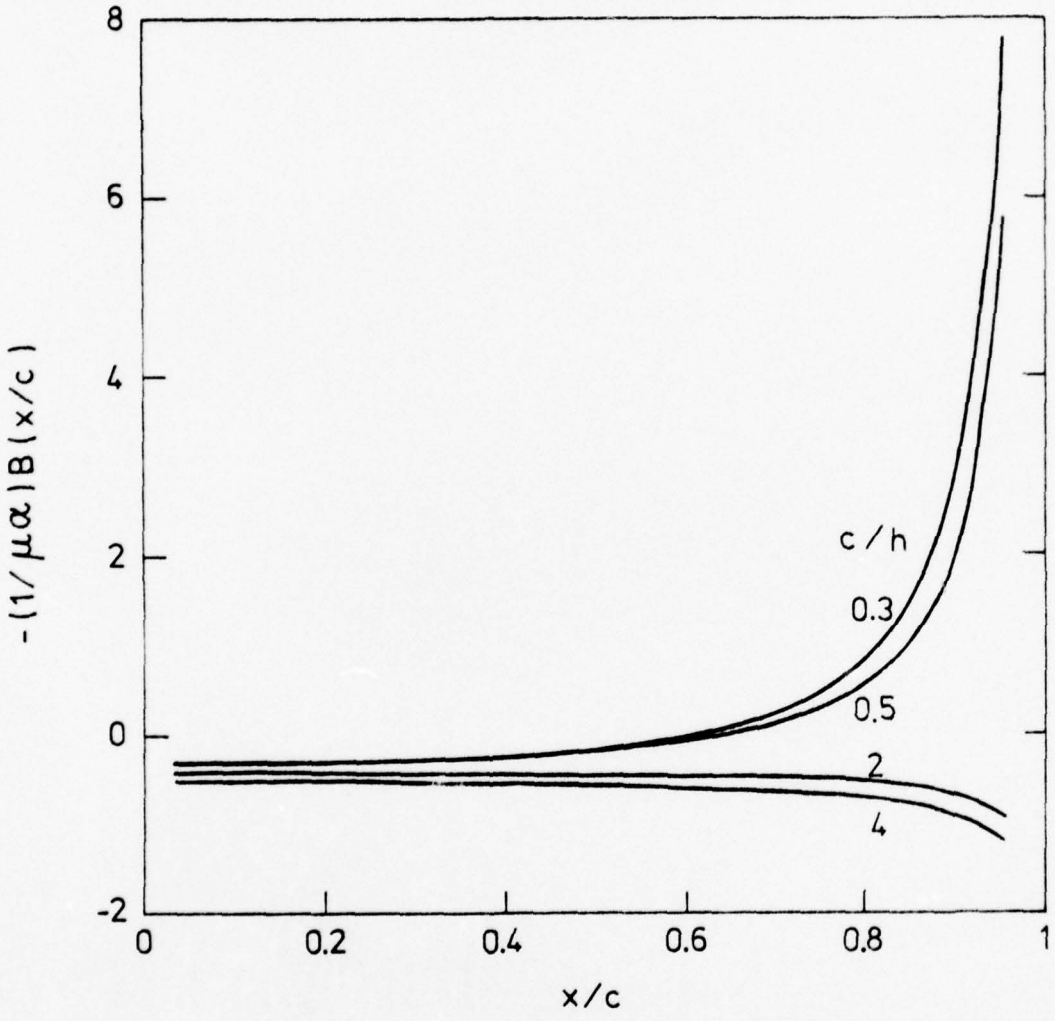

Fig. 14 Rotation: Shear stress distribution at y = h, 0 < x < c, for various values of c/h.

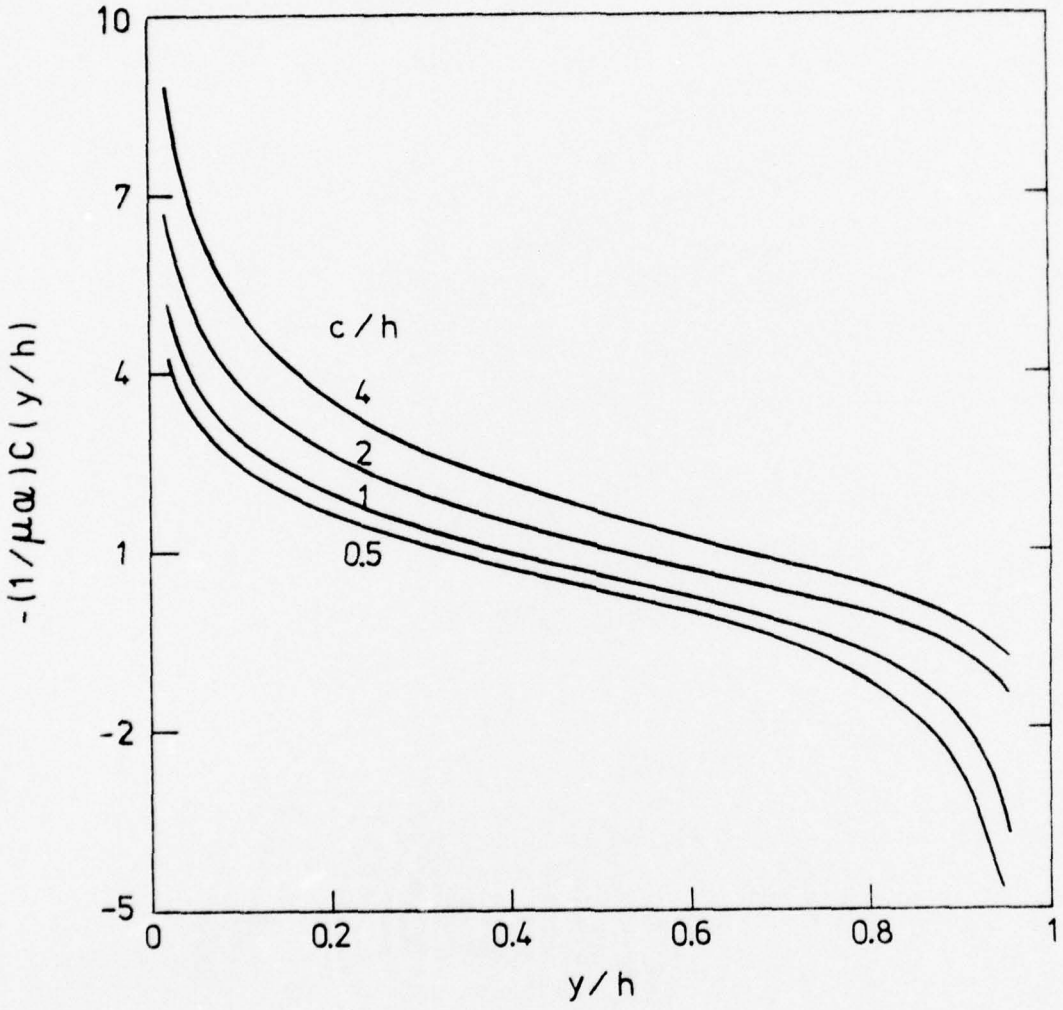

Fig. 15 Rotation; Normal stresses acting on the side of the block for $0 < y < h$, for several values of c/h.

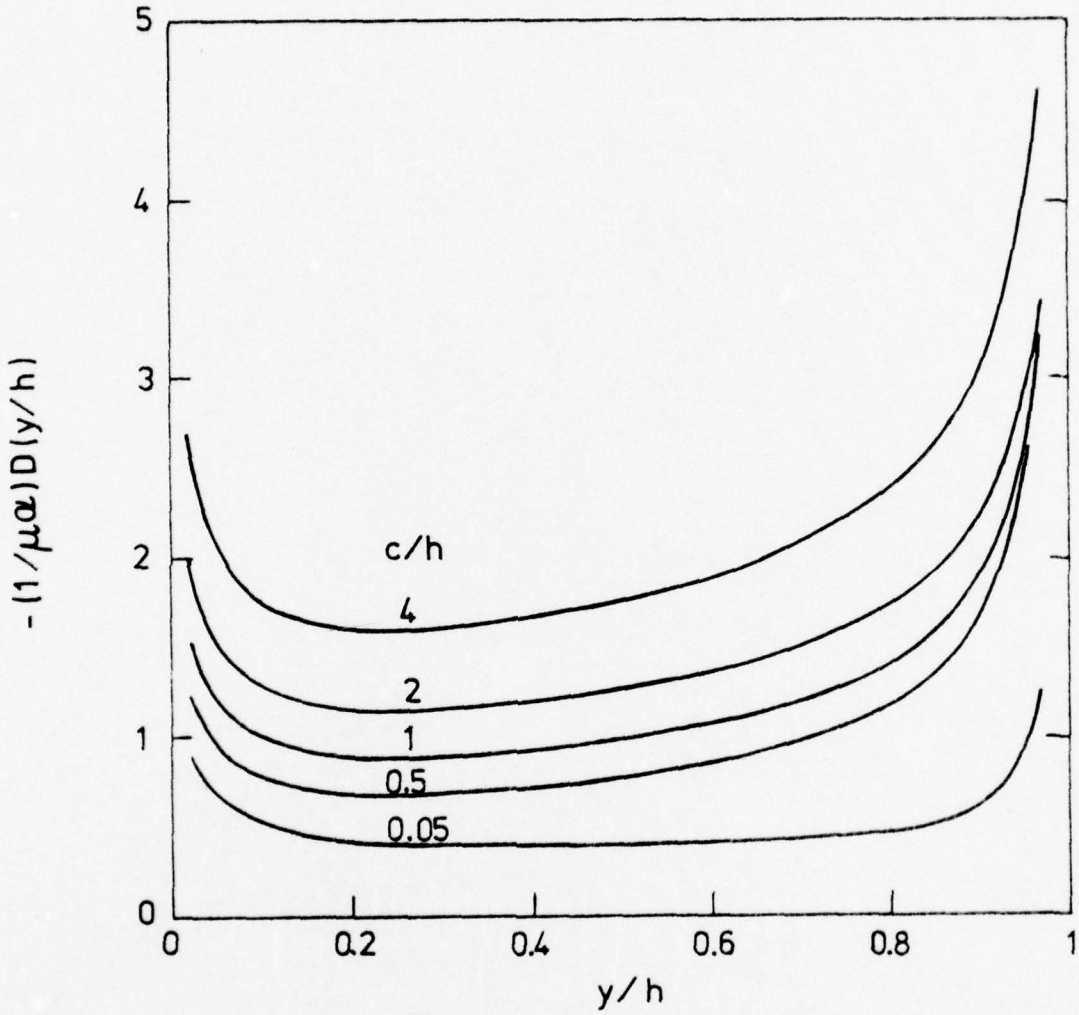

Fig. 16 Rotation: Shear stress distribution along the side of the block for $0 < y < h$, shown for several values of c/h.

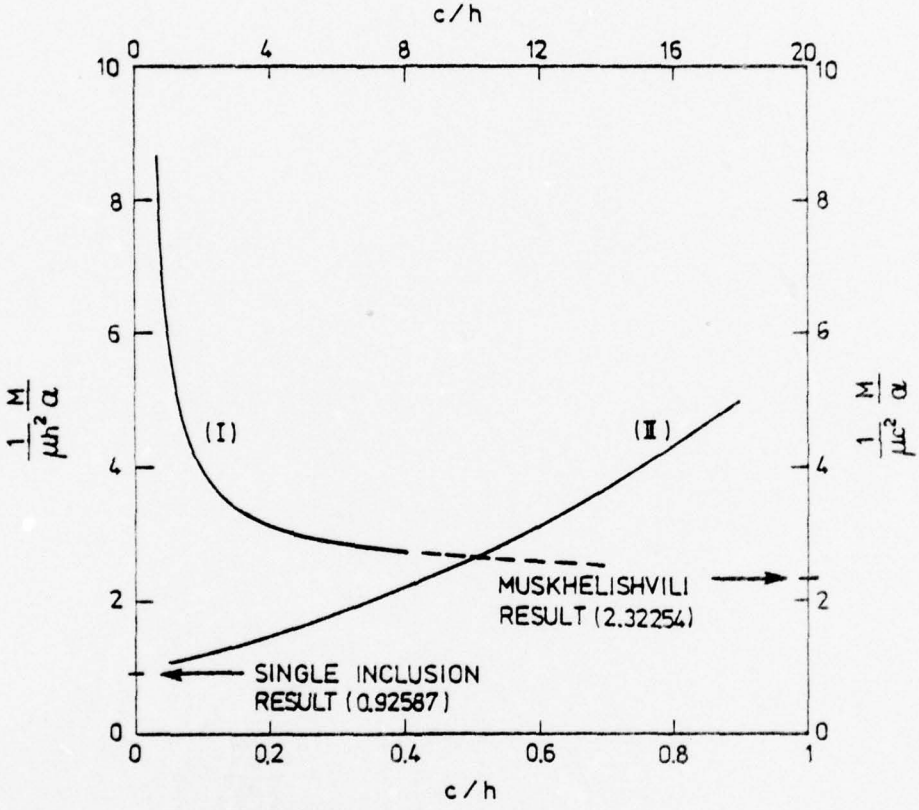

Fig. 17 Rotation: Stiffness for moment applied to rigid block (curve I: right ordinate, upper abscissa; curve II: left ordinate, lower abscissa).

APPENDIX A

The functions K_{Ni}, K_{Si}, L_{Ni}, and L_{Si}, $i = 1,2,\ldots,7$, are given as

$$K_{N1}(x,y;s) = \frac{2(h-y)[(h-y)^2-(x-s)^2]}{[(h-y)^2+(x-s)^2]^2} + \frac{(\kappa^2-1)(h+y)}{(h+y)^2+(x-s)^2} + \frac{2\kappa(h-y)[(h+y)^2-(x-s)^2]}{[(h+y)^2+(x-s)^2]^2} - \frac{8hy(h+y)[(h+y)^2-3(x-s)^2]}{[(h+y)^2+(x-s)^2]^3} \tag{A.1}$$

$$K_{S1}(x,y;s) = (x-s)\{\frac{2[(\kappa-2)(h-y)^2+\kappa(x-s)^2]}{[(h-y)^2+(x-s)^2]^2} + \frac{(\kappa^2+1)}{(h+y)^2+(x-s)^2} - \frac{4\kappa(h+y)^2}{[(h+y)^2+(x-s)^2]^2} + \frac{8hy[3(h+y)^2-(x-s)^2]}{[(h+y)^2+(x-s)^2]^3}\} \tag{A.2}$$

$$K_{N2}(x,y;s) = (x-s)\{\frac{2[(\kappa+2)(h-y)^2+\kappa(x-s)^2]}{[(h-y)^2+(x-s)^2]^2} + \frac{(\kappa^2+1)}{(h+y)^2+(x-s)^2} + \frac{4\kappa(h+y)^2}{[(h+y)^2+(x-s)^2]^2} + \frac{8hy[3(h+y)^2-(x-s)^2]}{[(h+y)^2+(x-s)^2]^3}\} \tag{A.3}$$

$$K_{S2}(x,y;s) = \frac{2(h-y)[(h-y)^2-(x-s)^2]}{[(h-y)^2+(x-s)^2]^2} - \frac{(\kappa^2-1)(h+y)}{(h+y)^2+(x-s)^2} + \frac{2\kappa(h-y)[(h+y)^2-(x-s)^2]}{[(h+y)^2+(x-s)^2]^2} + \frac{8hy(h+y)[(h+y)^2-3(x-s)^2]}{[(h+y)^2+(x-s)^2]^3} \tag{A.4}$$

$$K_{N3}(x,y;s) = (x-s)\{\frac{2[(h-y)^2-(x-s)^2]}{[(h-y)^2+(x-s)^2]^2} - \frac{(\kappa^2+2\kappa-1)}{(h+y)^2+(x-s)^2} - \frac{4(h+y)[2h+\kappa(h-y)]}{[(h+y)^2+(x-s)^2]^2} + \frac{8hy[3(h+y)^2-(x-s)^2]}{[(h+y)^2+(x-s)^2]^3}\} \tag{A.5}$$

$$K_{S3}(x,y;s) = -\frac{2(h-y)[\kappa(h-y)^2+(\kappa+2)(x-s)^2]}{[(h-y)^2+(x-s)^2]^2} + \frac{(\kappa+1)^2(h+y)}{(h+y)^2+(x-s)^2} - \frac{2[2h+\kappa(h+y)][(h+y)^2-(x-s)^2]}{[(h+y)^2+(x-s)^2]^2} + \frac{8hy(h+y)[(h+y)^2-3(x-s)^2]}{[(h+y)^2+(x-s)^2]^3} \tag{A.6}$$

$$K_{N4}(x,y;s) = -\frac{2(h-y)[\kappa(h-y)^2+(\kappa-2)(x-s)^2]}{[(h-y)^2+(x-s)^2]^2} + \frac{(\kappa-1)^2(h+y)}{(h+y)^2+(x-s)^2}$$

$$-\frac{2[2h-\kappa(h+y)][(h+y)^2-(x-s)^2]}{[(h+y)^2+(x-s)^2]^2} \qquad (A.7)$$

$$+\frac{8hy(h+y)[(h+y)^2-3(x-s)^2]}{[(h+y)^2+(x-s)^2]^3}$$

$$K_{S4}(x,y;s) = (x-s)\{\frac{2[(h-y)^2-(x-s)^2]}{[(h-y)^2+(x-s)^2]^2} + \frac{(\kappa^2-2\kappa-1)}{(h+y)^2+(x-s)^2}$$

$$+\frac{4(h+y)[2h-\kappa(h-y)]}{[(h+y)^2+(x-s)^2]^2} - \frac{8hy[3(h+y)^2-(x-s)^2]}{[(h+y)^2+(x-s)^2]^3}\} \qquad (A.8)$$

$$K_{N5}(x,y;s) = \frac{(h-y)[(\kappa-1)(h-y)^2-(5-\kappa)(x-s)^2]}{[(h-y)^2+(x-s)^2]^2} + \frac{(3\kappa-1)(h+y)}{(h+y)^2+(x-s)^2}$$

$$+\frac{2(3h-\kappa y)[(h+y)^2-(x-s)^2]}{[(h+y)^2+(x-s)^2]^2} - \frac{8hy(h+y)[(h+y)^2-3(x-s)^2]}{[(h+y)^2+(x-s)^2]^3} \qquad (A.9)$$

$$K_{S5}(x,y;s) = (x-s)\{\frac{[(\kappa-1)(h-y)^2+(3+\kappa)(x-s)^2]}{[(h-y)^2+(x-s)^2]^2} + \frac{(3\kappa+1)}{(h+y)^2+(x-s)^2}$$

$$-\frac{4(h+y)(3h+\kappa y)}{[(h+y)^2+(x-s)^2]^2} + \frac{8hy[3(h+y)^2-(x-s)^2]}{[(h+y)^2+(x-s)^2]^3}\} \qquad (A.10)$$

$$K_{N6}(x,y;s) = -\frac{(h-y)[(3+\kappa)(h-y)^2+(\kappa-1)(x-s)^2]}{[(h-y)^2+(x-s)^2]^2} + \frac{(\kappa+1)(h+y)}{(h+y)^2+(x-s)^2}$$

$$+\frac{2(h+\kappa y)[(h+y)^2-(x-s)^2]}{[(h+y)^2+(x-s)^2]^2} + \frac{8hy(h+y)[(h+y)^2-3(x-s)^2]}{[(h+y)^2+(x-s)^2]^3} \qquad (A.11)$$

$$K_{S6}(x,y;s) = (x-s)\{\frac{[(5-\kappa)(h-y)^2-(\kappa-1)(x-s)^2]}{[(h-y)^2+(x-s)^2]^2} + \frac{(\kappa-1)}{(h+y)^2+(x-s)^2}$$

$$-\frac{4(h+y)(h-\kappa y)}{[(h+y)^2+(x-s)^2]^2} - \frac{8hy[3(h+y)^2-(x-s)^2]}{[(h+y)^2+(x-s)^2]^3}\} \qquad (A.12)$$

$$K_{N7}(x,y;s) = (x-s)\{\frac{[(3+\kappa)(h-y)^2+(\kappa-1)(x-s)^2]}{[(h-y)^2+(x-s)^2]^2} - \frac{(\kappa-1)}{(h+y)^2+(x-s)^2}$$

$$-\frac{4(h+y)(h-\kappa y)}{[(h+y)^2+(x-s)^2]^2} + \frac{8hy[3(h+y)^2-(x-s)^2]}{[(h+y)^2+(x-s)^2]^3}\} \qquad (A.13)$$

$$K_{S7}(x,y;s) = -\frac{(h-y)[(\kappa-1)(h-y)^2+(3+\kappa)(x-s)^2]}{[(h-y)^2+(x-s)^2]^2} + \frac{(\kappa+1)(h+y)}{(h+y)^2+(x-s)^2}$$

$$-\frac{2(h+\kappa y)[(h+y)^2-(x-s)^2]}{[(h+y)^2+(x-s)^2]^2} + \frac{8hy(h+y)[(h+y)^2-3(x-s)^2]}{[(h+y)^2+(x-s)^2]^3} \tag{A.14}$$

$$L_{N1}(x,y;t) = (c-x)\left\{-\frac{2[(\kappa-2)(y-t)^2+\kappa(c-x)^2]}{[(y-t)^2+(c-x)^2]^2} - \frac{(\kappa^2+1)}{(y+t)^2+(c-x)^2}\right.$$

$$\left.+\frac{4\kappa(y+t)^2}{[(y+t)^2+(c-x)^2]^2} - \frac{8yt[3(y+t)^2-(c-x)^2]}{[(y+t)^2+(c-x)^2]^3}\right\} \tag{A.15}$$

$$L_{S1}(x,y;t) = -\frac{2(y-t)[(y-t)^2-(c-x)^2]}{[(y-t)^2+(c-x)^2]^2} + \frac{(\kappa^2-1)(y+t)}{(y+t)^2+(c-x)^2} \tag{A.16}$$

$$-\frac{2\kappa(y-t)[(y+t)^2-(c-x)^2]}{[(y+t)^2+(c-x)^2]^2} - \frac{8yt(y+t)[(y+t)^2-3(c-x)^2]}{[(y+t)^2+(c-x)^2]^3}$$

$$L_{N2}(x,y;t) = -\frac{2(y-t)[(y-t)^2-(c-x)^2]}{[(y-t)^2+(c-x)^2]^2} - \frac{(\kappa^2-1)(y+t)}{(y+t)^2+(c-x)^2} \tag{A.17}$$

$$-\frac{2\kappa(y-t)[(y+t)^2-(c-x)^2]}{[(y+t)^2+(c-x)^2]^2} + \frac{8yt(y+t)[(y+t)^2-3(c-x)^2]}{[(y+t)^2+(c-x)^2]^3}$$

$$L_{S2}(x,y;t) = (c-x)\left\{-\frac{2[(\kappa+2)(y-t)^2+\kappa(c-x)^2]}{[(y-t)^2+(c-x)^2]^2} - \frac{(\kappa^2+1)}{(y+t)^2+(c-x)^2}\right.$$

$$\left.-\frac{4\kappa(y+t)^2}{[(y+t)^2+(c-x)^2]^2} - \frac{8yt[3(y+t)^2-(c-x)^2]}{[(y+t)^2+(c-x)^2]^3}\right\} \tag{A.18}$$

$$L_{N3}(x,y;t) = \frac{2(y-t)[\kappa(y-t)^2+(\kappa+2)(c-x)^2]}{[(y-t)^2+(c-x)^2]^2} + \frac{(\kappa+1)^2(y+t)}{(y+t)^2+(c-x)^2}$$

$$-\frac{2[2t+\kappa(y+t)][(y+t)^2-(c-x)^2]}{[(y+t)^2+(c-x)^2]^2} \tag{A.19}$$

$$+\frac{8yt(y+t)[(y+t)^2-3(c-x)^2]}{[(y+t)^2+(c-x)^2]^3}$$

$$L_{S3}(x,y;t) = (c-x)\left\{-\frac{2[(y-t)^2-(c-x)^2]}{[(y-t)^2+(c-x)^2]^2} + \frac{(\kappa^2+2\kappa-1)}{(y+t)^2+(c-x)^2}\right.$$

$$\left.+\frac{4(y+t)[2t-\kappa(y-t)]}{[(y+t)^2+(c-x)^2]^2} - \frac{8yt[3(y+t)^2-(c-x)^2]}{[(y+t)^2+(c-x)^2]^3}\right\} \tag{A.20}$$

$$L_{N4}(x,y;t) = (c-x)\{-\frac{2[(y-t)^2-(c-x)^2]}{[(y-t)^2+(c-x)^2]^2} - \frac{(\kappa^2-2\kappa-1)}{(y+t)^2+(c-x)^2} \quad (A.21)$$

$$- \frac{4(y+t)[2t+\kappa(y-t)]}{[(y+t)^2+(c-x)^2]^2} + \frac{8yt[3(y+t)^2-(c-x)^2]}{[(y+t)^2+(c-x)^2]^3}\}$$

$$L_{S4}(x,y;t) = \frac{2(y-t)[\kappa(y-t)^2+(\kappa-2)(c-x)^2]}{[(y-t)^2+(c-x)^2]^2} + \frac{(\kappa-1)^2(y+t)}{(y+t)^2+(c-x)^2}$$

$$- \frac{2[2t-\kappa(y+t)][(y+t)^2-(c-x)^2]}{[(y+t)^2+(c-x)^2]^2} \quad (A.22)$$

$$+ \frac{8yt(y+t)[(y+t)^2-3(c-x)^2]}{[(y+t)^2+(c-x)^2]^3}$$

$$L_{N5}(x,y;t) = (c-x)\{-\frac{[(\kappa-1)(y-t)^2+(3+\kappa)(c-x)^2]}{[(y-t)^2+(c-x)^2]^2} - \frac{(3\kappa+1)}{(y+t)^2+(c-x)^2}$$

$$+ \frac{4(y+t)(3t+\kappa y)}{[(y+t)^2+(c-x)^2]^2} - \frac{8yt[3(y+t)^2-(c-x)^2]}{[(y+t)^2+(c-x)^2]^2}\} \quad (A.23)$$

$$L_{S5}(x,y;t) = -\frac{(y-t)[(\kappa-1)(y-t)^2-(5-\kappa)(c-x)^2]}{[(y-t)^2+(c-x)^2]^2} + \frac{(3\kappa-1)(y+t)}{(y+t)^2+(c-x)^2}$$

$$+ \frac{2(3t-\kappa y)[(y+t)^2-(c-x)^2]}{[(y+t)^2+(c-x)^2]^2} - \frac{8yt(y+t)[(y+t)^2-3(c-x)^2]}{[(y+t)^2+(c-x)^2]^3} \quad (A.24)$$

$$L_{N6}(x,y;t) = (c-x)\{-\frac{[(5-\kappa)(y-t)^2-(\kappa-1)(c-x)^2]}{[(y-t)^2+(c-x)^2]^2} - \frac{(\kappa-1)}{(y+t)^2+(c-x)^2}$$

$$+ \frac{4(y+t)(t-\kappa y)}{[(y+t)^2+(c-x)^2]^2} + \frac{8yt[3(y+t)^2-(c-x)^2]}{[(y+t)^2+(c-x)^2]^3}\} \quad (A.25)$$

$$L_{S6}(x,y;t) = \frac{(y-t)[(3+\kappa)(y-t)^2+(\kappa-1)(c-x)^2]}{[(y-t)^2+(c-x)^2]^2} + \frac{(\kappa+1)(y+t)}{(y+t)^2+(c-x)^2}$$

$$+ \frac{2(t+\kappa y)[(y+t)^2-(c-x)^2]}{[(y+t)^2+(c-x)^2]^2} + \frac{8yt(y+t)[(y+t)^2-3(c-x)^2]}{[(y+t)^2+(c-x)^2]^3} \quad (A.26)$$

$$L_{N7}(x,y;t) = \frac{(y-t)[(\kappa-1)(y-t)^2+(3+\kappa)(c-x)^2]}{[(y-t)^2+(c-x)^2]^2} + \frac{(\kappa+1)(y+t)}{(y+t)^2+(c-x)^2}$$

$$- \frac{2(t+\kappa y)[(y+t)^2-(c-x)^2]}{[(y+t)^2+(c-x)^2]^2} + \frac{8yt(y+t)[(y+t)^2-3(c-x)^2]}{[(y+t)^2+(c-x)^2]^3}$$

(A.27)

$$L_{S7}(x,y;t) = (c-x)\left\{-\frac{[(3+\kappa)(y-t)^2+(\kappa-1)(c-x)^2]}{[(y-t)^2+(c-x)^2]^2}+\frac{(\kappa-1)}{(y+t)^2+(c-x)^2}\right.$$

$$\left.+\frac{4(y+t)(t-\kappa y)}{[(y+t)^2+(c-x)^2]^2}-\frac{8yt[3(y+t)^2-(c-x)^2]}{[(y+t)^2+(c-x)^2]^3}\right\} \quad \text{(A.28)}$$

APPENDIX B

The calculated values of $\bar{A}$, $\bar{B}$, $\bar{C}$, and $\bar{D}$ at the corner (c,h), defined in Chapter VI, are given in this Appendix for various geometries.

The values given in Tables B1-B3 are based on the numerical results obtained from the solution of the problems formulated in Chapters III-V, respectively. These values were calculated by means of a quadratic extrapolation based on the three points nearest the corner (c,h).

The results presented in Tables B4-B6 are those obtained from the solution of the considered problems when three of the corner conditions are incorporated in the system of equations. Therefore, these results satisfy all corner conditions exactly.

As stated in Chapter VI the degree of accuracy of these results is unknown. However, the following general remarks can be made in association with these results. The corner conditions were derived by an asymptotic expansion of <u>all</u> singular terms appearing in the governing equations; this includes both the Cauchy-type kernels, and the terms of the generalized kernels with singular contributions near the end-points. Moreover, inclusion of the corner conditions in the system of equations introduces the proper interaction between the stress discontinuities in the vicinity of the corner (c,h). Also, as it was shown previously, inclusion of the corner conditions has little effect on the global results.

Therefore, it seems that including the corner conditions in the system of equations besides yielding correct global results, will also improve the accuracy of the results in the vicinity of the corners, provided that the difficulties discussed in Chapter VI have been successfully dealt with.

c/h	$\bar{A}(1)$	$\bar{B}(1)$	$\bar{C}(1)$	$\bar{D}(1)$
0.05	0.158	-0.157	0.203	0.153
0.1	0.163	-0.211	0.229	0.162
0.2	0.388	-0.314	0.278	-0.024
0.3	0.599	-0.316	0.192	-0.150
0.5	0.607	-0.253	0.089	-0.168
1	0.551	-0.295	0.144	-0.076
2	0.609	-0.265	0.079	0.012
4	0.678	-0.211	-0.010	0.039

TABLE B1 Vertical Displacement: Calculated values of $\bar{A}$, $\bar{B}$, $\bar{C}$, and $\bar{D}$ at the corner (c,h) for different geometries.

c/h	$\bar{A}(1)$	$\bar{B}(1)$	$\bar{C}(1)$	$\bar{D}(1)$
0.05	-0.107	0.364	-0.850	0.146
0.1	-0.222	0.569	-1.026	0.180
0.2	-0.356	0.779	-0.815	0.134
0.3	-0.273	0.661	-0.435	0.024
0.5	-0.136	0.183	0.199	-0.097
1	-0.150	0.011	0.368	-0.101
2	-0.240	0.440	0.029	-0.103
4	-0.305	0.604	0.040	-0.134

TABLE B2 Horizontal Displacement: Calculated values of $\bar{A}$, $\bar{B}$, $\bar{C}$, and $\bar{D}$ at the corner (c,h) for different geometries.

c/h	$\overline{A}(1)$	$\overline{B}(1)$	$\overline{C}(1)$	$\overline{D}(1)$
0.05	-3.630	-29.868	0.995	-0.244
0.1	5.164	-20.283	1.470	-0.349
0.2	7.262	-16.335	2.296	-0.617
0.3	5.207	-13.074	3.127	-0.866
0.5	2.303	-7.217	3.994	-1.088
1	0.216	-1.016	2.083	-0.536
2	-0.037	0.037	0.044	-0.200
4	-0.022	0.025	-0.022	-0.337

TABLE B3 Rotation: Calculated values of $\overline{A}$, $\overline{B}$, $\overline{C}$, and $\overline{D}$ at the corner (c,h) for different geometries.

c/h	$\bar{A}(1)$	$\bar{B}(1)$	$\bar{C}(1)$	$\bar{D}(1)$
0.05	0.123	-0.087	-0.445	0.316
0.1	0.144	-0.102	-0.346	0.246
0.2	0.139	-0.099	-0.222	0.157
0.3	0.134	-0.095	-0.167	0.119
0.5	0.131	-0.093	-0.121	0.086
1	0.158	-0.112	-0.097	0.069
2	0.186	-0.132	-0.075	0.053
4	0.182	-0.129	-0.049	0.035

TABLE B4 Vertical Displacement: Calculated values of $\bar{A}$, $\bar{B}$, $\bar{C}$, and $\bar{D}$ at the corner (c,h) for different geometries (using corner conditions).

c/h	$\overline{A}(1)$	$\overline{B}(1)$	$\overline{C}(1)$	$\overline{D}(1)$
0.05	-0.004	0.003	0.015	-0.010
0.1	-0.019	0.014	0.046	-0.033
0.2	-0.081	0.058	0.129	-0.092
0.3	-0.125	0.089	0.156	-0.111
0.5	-0.[illegible]	0.107	0.139	-0.098
1	-0.[illegible]82	0.129	0.111	-0.079
2	-0.327	0.232	0.132	-0.094
4	-0.569	0.404	0.152	-0.108

TABLE B5 Horizontal Displacement: Calculated values of $\overline{A}$, $\overline{B}$, $\overline{C}$, and $\overline{D}$ at the corner (c,h) for different geometries (using corner conditions).

c/h	$\bar{A}(1)$	$\bar{B}(1)$	$\bar{C}(1)$	$\bar{D}(1)$
0.05	-58.682	41.616	1.066	-0.756
0.1	-28.960	20.538	1.393	-0.988
0.2	-10.788	7.651	1.374	-0.974
0.3	-5.418	3.842	1.220	-0.865
0.5	-2.027	1.438	0.935	-0.663
1	-0.316	0.224	0.385	-0.273
2	-0.032	0.023	0.103	-0.073
4	-0.015	0.011	0.130	-0.092

TABLE B6 Rotation: Calculated values of $\bar{A}$, $\bar{B}$, $\bar{C}$, and $\bar{D}$ at the corner (c,h) for different geometries (using corner conditions).

BIBLIOGRAPHY

1. Muki, R., and Sternberg, E., "On the Diffusion of Load from a Transverse Tension Bar into a Semi-infinite Elastic Sheet," Journal of Applied Mechanics, Vol. 35, 1968, p. 737.
2. Reissner, E., "Note on the Problem of the Distribution of Stress in a Thin Stiffened Elastic Sheet," Proceedings of the National Academy of Sciences, Vol. 26, 1940, p. 300.
3. Muki, R., and Sternberg, E., "On the Diffusion of an Axial Load from an Infinite Cylindrical Bar Embedded in an Elastic Medium," Int. J. of Solids and Structures, Vol. 5, 1969, p. 587.
4. Muki, R., and Sternberg, E., "Elastostatic Load-Transfer to a Half-Space from a Partially Embedded Axially Loaded Rod," Int. J. of Solids and Structures, Vol. 6, 1970, p. 69.
5. Sneddon, I.N., "The Use of Integral Transforms," McGraw-Hill, New York, 1972.
6. Erdélyi, A., ed., "Tables of Integral Transforms," Vol. I, McGraw-Hill, New York, 1954.
7. Westmann, R.A., "Geometrical Effects in Adhesive Joints," Int. J. of Engineering Science, Vol. 13, 1975, p. 369.
8. Erdogan, F., Gupta, G.D., and Cook, T.S., "Numerical Solution of Singular Integral Equations," Methods of Analysis and Solutions to Crack Problems, ed., Sih, G.C., Noordhoff, 1972.
9. Williams, M.L., "Stress Singularities Resulting from Various Boundary Conditions in Angular Corners of Plates in Extension," Journal of Applied Mechanics, Vol. 19, TRANS. ASME, Vol. 74, 1952, p. 526.

10. Stroud, A.H., and Secrest, D., "Gaussian Quadrature Formulas," Prentice-Hall, Englewood Cliffs, N.J., 1966.

11. Abramowitz, M., and Stegun, I.A., "Handbook of Mathematical Functions," Dover, 1965.

12. Davis, P.J., "Interpolation and Approximation," Blaisdell Publishing Co., N.Y., 1965.

13. Muskhelishvili, N.I., "Some Basic Problems of the Mathematical Theory of Elasticity," Noordhoff, 1962.

14. Erdogan, F., and Gupta, G.D., "On the Numerical Solution of Singular Integral Equations," Quart. Appl. Math., Vol. 30, 1972, p. 525.

15. Kalandiya, A.I., "Mathematical Models of Two-Dimensional Elasticity," Mir Publishers, Moscow, 1975.

16. Theocaris, P.S., and Ioakimidis, N.I., "On the Numerical Evaluation of Stress Intensity Factors," Int. J. of Fracture, Vol. 12, 1976, p. 911.

17. Theocaris, P.S., and Ioakimidis, N.I., "Stress Intensity Factors and the Tips of an Antiplane Shear Crack Terminating at a Bimaterial Interface," Int. J. of Fracture, Vol. 13, 1977, p. 549.

18. Elliot, D., "Uniform Asymptotic Expansions of the Jacobi Polynomials and an Associated Function," Math. of Comp., Vol. 25, 1971, p. 309.

19. Erdogan, F., and Cook, T.S., "Antiplane Shear Crack Terminating At and Going Through a Bimaterial Interface," Int. J. of Fracture Vol. 10, 1974, p. 227.

VITA

NAME: George Konstantinos Haritos

BORN: 29 November 1947
Athens, Greece

EDUCATION: University of Illinois
Chicago, Illinois, 1965-1971

Northwestern University
Evanston, Illinois, 1975-1978

DEGREES: Bachelor of Science in Engineering
University of Illinois, 1969

Master of Science
University of Illinois, 1970

POSITION: Aeronautical Engineer-Structures
Aeronautical Systems Division
Wright-Patterson AF Base, Ohio, 1971-1975

AWARDS: Walter P. Murphy Fellowship
Northwestern University, 1975-1976